energies

MDPI

Article

Waste-to-Energy Conversion of Rubberwood Residues for Enhanced Biomass Fuels: Process Optimization and Eco-Efficiency Evaluation

Jannisa Kasawapat [1], Attaso Khamwichit [2,*] and Wipawee Dechapanya [2,*]

[1] Engineering Graduate Program, College of Graduate Studies, Walailak University, Thasala District, Nakhon Si Thammarat 80160, Thailand; jennisa.ka@mail.wu.ac.th
[2] Department of Chemical Engineering, School of Engineering and Technology, Walailak University, Thasala District, Nakhon Si Thammarat 80160, Thailand
* Correspondence: kattaso@mail.wu.ac.th (A.K.); khamwipawee@gmail.com (W.D.)

Abstract: Torrefaction was applied to enhance the fuel properties of sawdust (SD) and bark wood (BW), biomass wastes from the rubberwood processing industry. Design Expert (DE) software was used in an experimental design to study the effects of affecting factors including torrefaction temperature and time as well as the biomass size towards the desirable properties such as HHV, mass yield, fixed carbon content, and eco-efficiency values. Promising results showed that the HHVs of the torrefied SD (25 MJ/kg) and BW (26 MJ/kg) were significantly increased when compared to preheated SD (17 MJ/kg) and preheated BW (17 MJ/kg) and in a range similar to that of coal (25–35 MJ/kg). The TGA, FTIR, biomass compositions, and O/C ratios suggested that thermochemical reactions played a significant role in the torrefaction at which thermal degradation coupled with possible in situ chemical reactions took place, to some extent. The optimal conditions of the torrefaction were identified at 320 °C and 30 min for SD, and 325 °C and 30 min for BW. The maximum HHVs at the optimal condition were 22, 23, and 20 MJ/kg while the eco-efficiency values were 29.18, 27.89, and 13.72 kJ/kg CO_{2_eq}*THB for torrefied SD, torrefied BW, and coal, respectively. The findings of this study indicate that torrefied rubberwood residues enhanced HHV, eco-efficiency, and less contribution to CO_2 emissions compared to fossil fuels.

Keywords: waste-to-energy; biomass valorization; bioenergy; torrefaction; CO_2 emissions

check for updates

Citation: Kasawapat, J.; Khamwichit, A.; Dechapanya, W. Waste-to-Energy Conversion of Rubberwood Residues for Enhanced Biomass Fuels: Process Optimization and Eco-Efficiency Evaluation. *Energies* **2024**, *17*, 5444. https://doi.org/10.3390/en17215444

Academic Editor: Wojciech Jerzak

Received: 21 September 2024
Revised: 23 October 2024
Accepted: 28 October 2024
Published: 31 October 2024

Copyright: © 2024 by the authors. Licensee MDPI, Basel, Switzerland. This article is an open access article distributed under the terms and conditions of the Creative Commons Attribution (CC BY) license (https://creativecommons.org/licenses/by/4.0/).

1. Introduction

The main energy source powering the world economy is fossil fuels. However, they have several disadvantages that affect energy stability, global warming, and climate change, such as large CO_2 emissions, price volatility, and resource depletion [1]. Countries worldwide are looking for renewable and alternative energy sources to lessen their dependency on fossil fuels [2]. The potential for renewable and alternative energy resources varies by country due to geography, climate, lifestyle, and agro-industrial activity. The higher heating value (HHV) of coal typically ranges from 25 to 35 MJ/kg, depending on its rank and type [3]; e.g., anthracite (33.58 MJ/kg) [4], bituminous (26.89 MJ/kg), sub-bituminous (25.31 MJ/kg) [5], and lignite (24.98 MJ/kg) [6]. However, coal combustion results in significant emissions of carbon dioxide (CO_2), sulfur dioxide (SO_2), nitrogen oxides (NOx), and particulate matter (PM) [7]. These emissions pose considerable environmental and health concerns, necessitating careful consideration in energy policy and industrial applications. In contrast, biomass exhibits a lower HHV range of approximately 15–20 MJ/kg but emits less SO_2 and NOx [8]. Regarding the superior HHV of coal (25–35 MJ/kg) compared to that of biomass (17 MJ/kg), torrefaction was applied to enhance the HHV of torrefied biomass. Torrefied biomass, which is biomass that has been thermally processed, has an HHV of approximately 20–24 MJ/kg [9]. It emits fewer pollutants than coal, with reduced moisture

content and improved combustion efficiency, making it a more sustainable and efficient alternative to both coal and untreated biomass [10]. Torrefied biomass demonstrates superior environmental performance compared to coal in terms of pollutant emissions [11]. The lower sulfur content in torrefied biomass results in a substantial reduction of sulfur dioxide (SO_2) emissions, a primary cause of acid rain. Furthermore, the decreased nitrogen content and simpler hydrocarbon structure of torrefied biomass lead to lower emissions of nitrogen oxides (NO_x) and volatile organic compounds (VOCs) [12]. The combustion characteristics of torrefied biomass also contribute to a more complete and efficient burn, thereby minimizing particulate matter (PM) emissions. These factors collectively position torrefied biomass as a more environmentally sustainable alternative to coal in terms of emissions profile and carbon impact [13]. Furthermore, the significantly lower moisture content of torrefied biomass indicates an enhanced energy efficiency, as less energy is expended on water evaporation. Consequently, torrefied biomass demonstrates an improved heat production efficiency relative to coal, positioning it as a promising alternative fuel source in industrial applications [14]. It also holds the potential for enhancing carbon neutrality in various industrial processes. For example, torrefied biomass has been utilized for energy generation through co-firing technology in the steel, pulp, and paper industries. The leverage of biomass fuels not only reduces their reliance on fossil fuels but also improves the overall energy efficiency of the process [15,16]. Growing demand for this biofuel is probably going to spur improvements in supply chain logistics, which will ultimately strengthen the market for renewable energy sources [17].

The economy of Thailand relies heavily on tourism, with the agro-industrial and manufacturing sectors also playing significant roles. Major agricultural products include cassava, rice, palm oil, and natural rubber. The cultivation, harvesting, and processing of these products yield substantial amounts of solid biomass. In particular, rubber trees and oil palm plantations are prevalent in the southern country peninsula. In 2022, approximately 3.85 million hectares of rubber were planted in Thailand [18], accounting for 58% of agricultural growth in the southern area. Natural rubber latex can typically be harvested from a planted rubber tree for 25 to 30 years. At the end of this cycle, replanting is necessary, generating various forms of biomass from the roots, trunks, and branches, estimated at roughly 13, 250, and 74 tonnes per hectare, respectively [19]. Traditionally, rubberwood lumber is produced by processing appropriately sized trunks, which also generate by-products such as sawdust, bark, and slabs. Additionally, these biomass and roots are converted into woodchips, which are used as solid fuels in factories and biomass power plants. Sawdust is commonly utilized in pellet production and the mushroom cultivation industry. Despite their widespread use in various forms of solid fuels for heat and electricity production, the potential for these biomass resources remains significant [20].

Wood biomass ranks among the most abundant biomass materials, widely utilized for the production of renewable bioenergy, high-value chemicals, and materials. Southern Thailand is the primary region for rubber cultivation, encompassing the majority of the regions of the nation that grow rubber. This region has a planting area of approximately 7–8 million rai, producing around 3–4 million tonnes of rubber annually [21]. Oil palm is another significant economic crop in the southern region, with a planting area of approximately 4–5 million rai and an annual production of 15–18 million tonnes of oil palm fruit [22]. The amount of waste and product generated from processing rubberwood varies depending on the management of the factory and production methods. Consequently, the distribution of wood processing is as follows: primary products account for 50–60%, and total waste accounts for 40–50% [23]. Waste components include bark wood, which accounts for about 10–15%; sawdust, at 10–20%; wood dust, at 10%; and wood chips and branches, at 30%. The price of bark wood ranges from 1500 to 3000 baht per tonne [24], while the price of sawdust ranges from 700 to 1500 baht per tonne [24], depending on the quality, market demand, and region. The disadvantages of raw biomass involve high moisture content, high hygroscopicity, low bulk density, low HHV, elevated ash content, reduced carbon content, and poor grindability [13]. Hence, specific approaches and technologies are needed

to lessen their effects and guarantee effective biomass management through the supply chain. The torrefaction process is an effective method to address these issues [3].

Biomass torrefaction is increasingly recognized as a crucial preprocessing technique to enhance the quality of biomass in terms of physical properties and chemical composition. Torrefaction involves the gradual heating of biomass in an inert or reduced-oxygen environment to a maximum temperature of approximately 200–300 °C [25] for a duration time of 30–120 min [16]. During this process, key components of biomass, particularly hemicellulose, undergo degradation through depolymerization, demethylation, bond cleavage, and condensation reactions. These reactions result in the removal of moisture and some volatile compounds. Torrefaction significantly improves the HHV and hydrophobicity of biomass, while also reducing its susceptibility to fungal and microbial degradation [26]. The process has been demonstrated to enhance wood quality for thermo-chemical conversion, improve size reduction characteristics, increase the HHV of biomass, achieve high process efficiency (94%), and produce a coal-like fuel [27]. The price of torrefied biomass can vary depending on factors such as product quality, production process, market demand, and sales location. Generally, the price of torrefied biomass from rubberwood ranges between approximately 5000 and 8000 THB per tonne [24].

The thermogravimetric analysis (TGA) and Fourier transform infrared spectroscopy (FTIR) analysis can give insight into the thermal degradation and chemical changes of the biomass, caused by thermochemical reactions that are taking place during the torrefaction process [28]. It was discovered that lignin breakdown and cellulose cross-linking during torrefaction were subordinated to the thermal breakdown of carbohydrates, primarily, hemicellulose. According to a previous study [29], several reactions take place during the torrefaction process of raw biomass, resulting in an increased HHV of the torrefied biomass, decreased oxygen content, increased carbon content, and improved grind ability. Additionally, the torrefied biomass exhibits hydrophobic characteristics [30]. In all cases, both mass and energy yields decrease as torrefaction temperature or time increases, indicating a trade-off between improved fuel quality and mass and energy retention. Significant interest in upgrading torrefied wood as solid fuel has also been growing throughout the decade, with several studies investigating topics such as wood characteristics as raw materials, torrefied qualities, torrefying conditions, storage characteristics, combustion properties, and pre-treatment [31].

The utilization of torrefied biomass as a fuel alternative presents notable environmental advantages, particularly in the aspect of lowering greenhouse gas emissions [32]. The production of biomass fuel by torrefaction enables the transformation of low-value bio waste into high-value biofuel [33]. This value-added approach not only addresses waste management challenges but also creates new economic opportunities within the renewable energy sector. However, the initial investment costs of process upgrading that requires specialized equipment and know-how of the optimal conditions to carry out the torrefaction process effectively could be the drawbacks to be considered [34]. Nevertheless, the integration of torrefied biomass into existing energy systems can be a viable approach that eventually leads to significant energy security enhancement by diversifying the fuel sources. As countries seek to reduce their reliance on fossil fuels, utilizing torrefied biomass not only contributes to a circular economy but also aligns with international sustainability goals, such as those set by the United Nations for low carbon emissions [35].

Despite the extensive research on biomass torrefaction, the application of Design Expert (DE) software remains underutilized in this field. This study addresses this gap by leveraging DE to identify and evaluate the impact of various parameters, enabling the development of precise statistical models, minimizing the number of required experiments, and expediting the process of determining optimal conditions. The research focuses on two critical aspects: firstly, a comprehensive analysis of factors influencing the torrefaction process, including torrefaction temperature, biomass particle size, and torrefaction time; and secondly, the simultaneous optimization of four key responses: HHV, mass yield, fixed carbon content, and eco-efficiency. This approach provides a robust framework

for advancing the understanding and optimization of biomass torrefaction processes, contributing valuable insights to renewable energy and sustainable resource management.

2. Materials and Methods

Rubberwood bark wood and sawdust residues underwent torrefaction. The resulting products were analyzed for chemical structure, composition, thermal degradation, and fuel properties. Process performance and eco-efficiency were assessed to evaluate potential. Statistical analysis identified relationships between key parameters and properties to determine the optimal process conditions. Details are as follows:

2.1. Sample Preparation

Khao Mahachai Parawood Company Limited, Nakhon Si Thammarat, Thailand was the source of the bark wood (BW) and sawdust (SD) residues used in this study. Timber bandsaws (BIGWOOD BS-12N) were used to cut BW into segments of wood in three different sizes: 5 mm, 7.5 mm, and 10 mm. By utilizing sieves with apertures of 0.5 mm (number 30 sieve), 0.85 mm (number 20 sieve), and 1.0 mm (number 18 sieve), SD was ground and sieved by ASTM E11 [36] and according to the International ISO 565 standards [37]. The results passed grided BW and SD samples were next dried for 24 h at 105 °C in a hot air oven (Model UM-500; Memlert, Germany) and kept at room temperature within a desiccator (Model RT-48C; Eureka Design Co., Ltd., Pathum Thani, Thailand).

2.2. Torrefaction Process

Before torrefaction, the feedstock moisture content was lowered in the preheating process using a hot air oven (BW decreased from 38.86 wt.% to 12.32 wt.% and SD decreased from 34.34 wt.% to 10.11 wt.% on a wet basis). A ceramic reactor with a sealed cover was filled with 50 g of the preheated biomass mentioned above to begin the torrefaction process. The reactor, as shown in Figure 1, was put inside a furnace (Carbolite Gero Ltd., Parsons Lane, United Kingdom; type AAF11/3), with the temperature set to the appropriate levels for torrefaction (200, 250, 275, 300, and 350 °C). To investigate the torrefaction times of 30, 75, and 120 min, the torrefaction process was carried out at a heating rate of less than 40 °C/min while keeping a constant temperature for the duration. Once the samples had reached ambient temperature, they were removed from the furnace and set inside a desiccator (Model RT-48C; Eureka Design Co., Ltd.; Pathum Thani, Thailand) for further characterization.

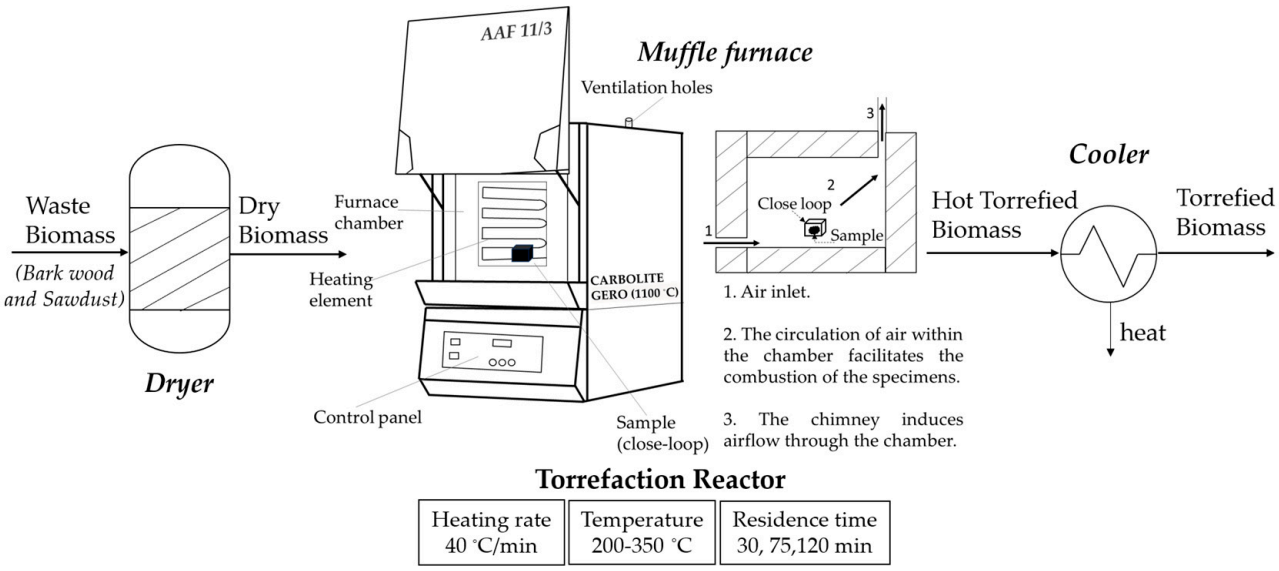


Figure 1. Schematic diagram of the torrefaction process.

2.3. Characterization

Three repetitions were employed in the experiments for all the characterization analyses of the samples.

2.3.1. Proximate Analysis

The moisture content (MC), volatile matters (VM), ash content (AC), and fixed carbon contents (FC) were analyzed by the proximate analysis. Analyses of MC, AC, and VM were performed based on ASTM E871; The Standard Test Method Moisture Analysis. ASTM International: PA, USA, 2019, ASTM E830; The Standard Test Method for Ash in the Analysis Sample of Refuse-Derived Fuel. ASTM International, Pennsylvania, USA, 2004, and ASTM E872; The Standard Test Method for Volatile Matter in the Analysis of Particulate Wood Fuels. ASTM International, Pennsylvania, USA, 2019. correspondingly. The average results from the proximate analysis were presented in weight percentage of moisture-free basis (mf wt.%). The FC was calculated from Equation (1).

$$\text{FC (mf wt.\%)} = 100 - [\text{VM} + \text{AC}] \text{ (mf wt.\%)} \quad (1)$$

2.3.2. Higher Heating Value

The HHV was determined using a Bomb Calorimeter (model LECO AC500; LECO Corporation, MI, USA) following the standard test procedure ASTM E711; The Standard Test Method for Gross Calorific Value of Refuse-Derived Fuel by the Bomb Calorimeter. ASTM International: Pennsylvania, United States, 2004. The schematic of the Bomb Calorimeter is illustrated in Figure 2. Before sample analysis, calibration of the calorimeter was performed using benzoic acid. Subsequently, a dried sample of 1 g was introduced into the calorimeter equipment and combusted in an oxygen (O_2) atmosphere at a pressure of 3000 kPa. The ignition wire length was recorded. After combustion, the resulting 10.45 g of sodium carbonate per 500 mL of DI water was used to titrate the solution until the color of the mixture transformed from pink to light orange, as shown by methyl orange. To calculate the sample calorific value, the Tesco AC500 software (Automation Builder version 2.7.0) was used to enter the length of the ignition wire and the amount of titrant utilized.

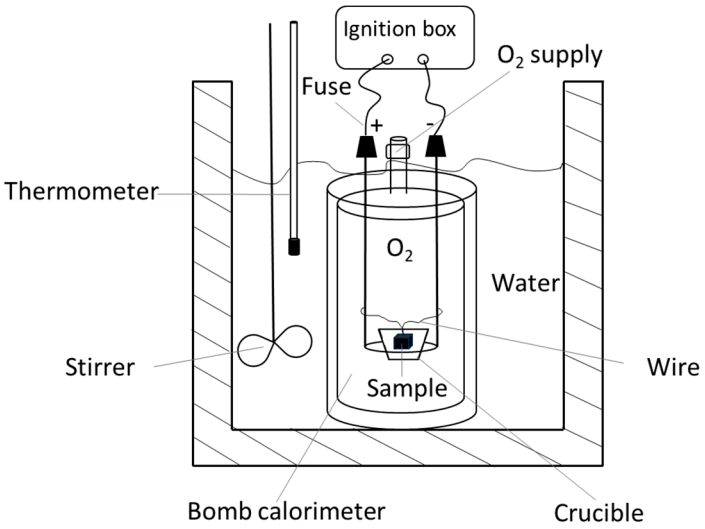


Figure 2. Bomb Calorimeter.

2.3.3. Analysis of Production Yield and Energy Densification Ratio

The mass yield (Y_M) and energy efficiency (E_E) are assessed as critical markers of a torrefaction process. They show how much energy is held in the solid product during torrefaction and how much dry mass is lost. The definitions of these indicators are shown in Equations (2)–(4). A very important factor for a process is its overall energy densification

ratio (EDR), which is normally used to evaluate the proficiency of a process in terms of using energy [38].

$$Y_M\ (\%) = \frac{mass_{torrefaction}}{mass_{raw\ biomass}} \times 100\% \quad (2)$$

$$E_E\ (\%) = EDR \times \%\ Y_M \quad (3)$$

$$EDR = \frac{E_E}{Y_M} = \frac{HHV_{torrefaction}}{HHV_{raw\ biomass}} \quad (4)$$

2.3.4. Thermogravimetric Analysis (TGA)

Preheated BW and SD were measured to 10 mg and then added to the sample pan of the TGA/GCMS device. The analysis was carried out in a nitrogen environment while maintaining a flow rate of 20 mL/min to avoid oxidation. The temperature was increased at a rate of 10 °C/min from 25 °C to 800 °C. The mass of the BW and SD was constantly measured as the temperature rose, gathering information on moisture loss and the breakdown of cellulose, hemicellulose, and lignin.

2.3.5. Lignocellulose Analysis of Torrefied BW and SD

An essential method for understanding the composition of biomass is the analysis of lignocellulose, according to the National Renewable Energy Laboratory (NREL) version 08–03–2012, which includes cellulose, lignin, and hemicellulose [39]. To perform this analysis, 80 cm^3 of acetone was used to extract 5 g of preheated BW and SD (at 105 °C for 24 h) in a Soxhlet extractor (Foss Soxtec^{TM} 2050; Foss Tecator AB, Hoganas, Sweden) at 90 °C for 1 h. The BW and SD were then allowed to cool down to room temperature and rinsed with fresh acetone for 30 min. Consequently, once the weight remained consistent, the biomass residues were collected and oven-dried at 105 °C. The acetone extractable content of biomass E (%) was calculated by Equation (5).

$$E\ (\%) = \left[\frac{(W_0 - W_1)}{W_0}\right] \times 100\% \quad (5)$$

where W_0 and W_1 represent the weight in dry terms of the torrefied biomass both before and following extraction.

The amount of hemicellulose was measured by adding 3 cm^3 of sodium hydroxide solution (0.5 mol dm^{-3}) to 0.3 g of pre-extracted sample, as previously described, in a 15 cm^3 test tube. The mixture was heated to boiling at 80 °C for 3.5 h. After cooling to room temperature, the mixture was vacuum filtered using Whatman no. 1 filter paper. After that, distilled water was used to completely rinse the solid residue until it reached a neutral pH of 7. Subsequently, the leftover material was dehydrated at 105 °C until a consistent weight was attained, then cooled in a desiccator and weighed. Hemicellulose content H (%) was calculated using the following equation.

$$H\ (\%) = \left[\frac{(W_1 - W_2)}{W_1}\right] \times 100\% \quad (6)$$

where W_2 is the weight in dry terms following the application of alkali.

A pre-weighed flask containing 0.2 g of biomass extracted by acetone was used to measure the lignin content. The chemicals used in the test include acetone (99.5% pure by AR grade), sodium hydroxide (99% pure by AR grade), and sulfuric acid (98 percent pure by AR grade) were purchased from RCI Laboratories (Bangkok, Thailand). Sulfuric acid with the amounts of 200 cm^3 and 720 g of H_2SO_4 dm^{-3} was gradually added at 30 °C to the flask for 1 h. Afterward, 56 cm^3 of distilled water was added. The flask was put into the autoclave at 121 °C for 1 h. After bringing the flask contents to the ambient temperature, Whatman No. 1 filter paper was used to filter the solution. To ensure that there was no sulfate in the filtrate, the residues were cleaned with distilled water until the water turned

clear. The filtrated residues were then weighed after 3 h of oven drying at 105 °C [40]. The lignin content L (%) was estimated using Equation (7).

$$L\ (\%) = (W_4/W_3) \times 100\% \quad (7)$$

where W_3 is the sample mass before treatment is indicated and W_4 represents the mass of the solids obtained after the treatment.

Judging from the torrefied biomass extracted with acetone, the cellulose content (expressed as C %) was determined using Equation (8).

$$C\ (\%) = 100 - H\ (\%) - L\ (\%) \quad (8)$$

2.3.6. Fourier Transform Infrared (FTIR) Analysis

FTIR spectra of the samples were examined to gain a deeper insight into how the torrefaction process impacts the chemical structure through thermal effects. To perform this analysis, 1 g of preheated sample was employed in ATR–FTIR of BW and KBr–FTIR of SD. An FTIR spectrometer was employed to analyze the FTIR spectra of the materials (Tensor 27 model; Bruker, Ettlingen, Germany) between 530 and 4000 cm^{-1} in wavelength.

2.3.7. Scanning Electron Microscopy (SEM)/EDX

An SEM (Carl Zeiss Co., Ltd., Bangkok, Thailand; Model Merlin Compact) was performed to examine the morphological properties of the samples. The preheated torrefied biomass was placed on a carbon stub, gold sputtering was carried out, and the outcomes were examined with a Jeol Jx A-840 SEM (Jeol, MA, USA). Images captured by the SEM images were analyzed with the MicroSun 2000/s image analysis software (version 2.0) to collect nano structural data of the torrefied biomass. The magnification of the picture analysis was 500× at 5 kV.

2.4. Eco-Efficiency Analysis

Eco-efficiency is a useful instrument for promoting sustainable development and respects ISO 14045; Environmental management—Eco-efficiency assessment of product systems—Principles, requirements and guidelines. ISO: Geneva, Switzerland, 2012. as a standard for evaluating the eco-efficiency of product systems within Environmental Management [41]. By incorporating factors like resource usage, economic development, and environmental effects, eco-efficiency provides a complete measure for assessing how well product, process, and service (PPS) systems are performing [42]. It is described as the relationship between the value of a product or service and its effects on the environment, encompassing factors such as the consumption of materials, energy, and water, along with greenhouse gas and carbon dioxide emissions. The conceptual equation for calculating ecoefficiency is presented as Equation (9) [42].

$$\text{Eco} - \text{efficiency} = \frac{\text{Value of the product, process, or service (PPS)}}{\text{Environmental impact of the PPS}} \quad (9)$$

This concept was employed in this study. The value of the torrefied biomass was interpreted in terms of HHV, the desired property of the material to be used as biofuel. In the aspect of environmental impact, the CO_2 equivalent emission is caused by the complete combustion of the biomass itself when used for energy generation.

The carbon storage (CS) of the torrefied biomass was estimated from the fixed carbon content of the biomass, as shown in Equation (10). When the material undergoes thermal decomposition, this solid carbon in the wood is released again into the atmosphere as CO_2 gas. It is to be noted that the carbon is trapped as a solid and does not contribute to climate change through the atmospheric greenhouse effect as long as the wood is contained within a biomass. By multiplying the carbon content of a specific torrefied biomass by the ratio

of the molecular weight of CO_2 and C, it was possible to determine the amount of carbon stored per unit of biomass [43].

$$\text{CS (kg } CO_{2_eq}\text{/kg biomass)} = CC_{\text{torrefied biomass}} \times 3.67 \quad (10)$$

where:

CS = carbon storage which is converted to CO_2 equivalent per unit of biomass (kg CO_{2_eq}/kg biomass)

CC torrefied biomass = FC content torrefied biomass − FC content raw biomass (% carbon),

3.67 = ratio of the molecular weight of CO_2 to the molecular weight of C.

Emitted CO_2 of torrefied biomass (CBB) occurs when wood is combusted for energy, in which burning biomass emits CO_2 0.0918 kg CO_2/MJ (bone dry) [44]. The conceptual equation for calculating carbon emissions is presented in Equation (11).

$$\text{CBB (kg } CO_{2_eq}\text{/kg biomass)} = \text{HHV (MJ/kg biomass)} \times 0.0918 \text{ (kg } CO_{2_eq}\text{/MJ)} \quad (11)$$

Total CO_2 equivalent (fCO_2) emissions of torrefied biomass include carbon storage in biomass, which is converted to CO_{2_eq}, and the emitted CO_2 from a torrefaction process. Total CO_2 equivalent emission is estimated using the following equation.

$$CO_{2_eq} \text{ (kg } CO_{2_eq}\text{/kg biomass)} = \text{CS} + \text{CBB} \quad (12)$$

Integrating the concepts of sustainability and eco-efficiency in the present study necessitated an adaptation of the eco-efficiency Equation (9) for the eco-efficiency calculation, as follows in Equation (13).

$$\text{Eco} - \text{efficiency} = \frac{\text{HHV}\left(\frac{\text{kJ}}{\text{kg biomass}}\right)}{CO_{2_eq}\left(\frac{\text{kg } CO_{2_eq}}{\text{kg biomass}}\right) \times \text{Cost (THB)}} \quad (13)$$

where CO_2 equivalent (CO_{2_eq}) was estimated from Equations (11) and (12) [43,44].

The cost of torrefied biomass used in Equation (13) comprised the fixed and operating costs. The fixed cost was determined using the costs related to the acquisition and gridding of biomass. Both chemical and electricity costs were included in the overall operating cost of the torrefaction process.

2.5. Design Experimentation

The Design–Expert® (DE) software edition 13 (Stat–Ease, Inc., Minneapolis, MN, USA) was used in this study to provide tools such as experimental design, response surface methodology (RSM), and statistical analysis including ANOVA and regression. The key affecting parameters (inputs) included torrefaction temperature, torrefaction time, and biomass particle size. The study focused on four response variables: maximum HHV, %mass yield, %FC, and eco-efficiency. Thirty trial runs of each form of biomass were produced by running the DE program.

3. Results

The detailed discussions include the characterization results, process performance and eco-efficiency analysis, and process optimization as follows:

3.1. Preparation of Torrefied BW and SD

Following a 24 h drying process in a hot air oven at 105 °C to remove moisture, the biomass is prepared for torrefaction by placing it in a muffle furnace. Enhancing the chemical and physical properties of the biomass is the aim of this process. Temperatures between 200 °C and 350 °C were used in the torrefaction process with a predefined period.

The physical characteristics of the torrefied materials changed dramatically, specifically, the initial color of the raw material was either light brown, orange, or golden, as seen in Figure 3. But the colors of the material gradually darkened, transitioning from light brown to dark brown and, ultimately, to dark as the torrefaction process temperature rose. Interestingly, the residual biomass showed a characteristic black color at 350 °C.

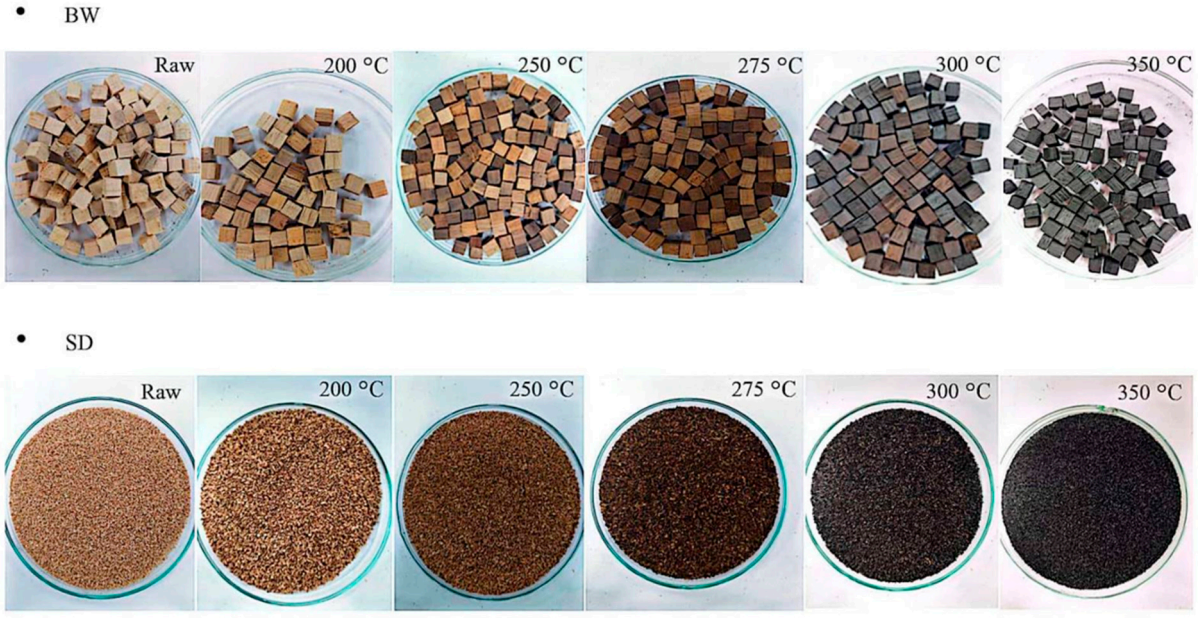


Figure 3. The physical appearance of the raw and torrefied BW and SD samples at different temperatures.

3.2. Biomass Characterization

3.2.1. Proximate Analysis Results

Figure 4 shows the moisture content (MC) of the biomass samples before and after torrefaction. The MC of the untreated biomass was 34.34% for SD and 38.86% for BW. Relative humidity dropped to 11.15% and 9.17% for BW and SD, respectively, during the pretreatment procedure. The moisture level significantly decreased during the torrefaction process, reducing to 1–3% for BW and SD. This implied that the temperature during the torrefaction process hurts moisture content. The moisture content of biomass is one of the main factors causing its poor fuel characteristics; lower moisture content results in biomass with an HHV. According to [45], dehydration results in a decrease in biomass moisture content, which, in turn, causes the material to lose a portion of its weight.

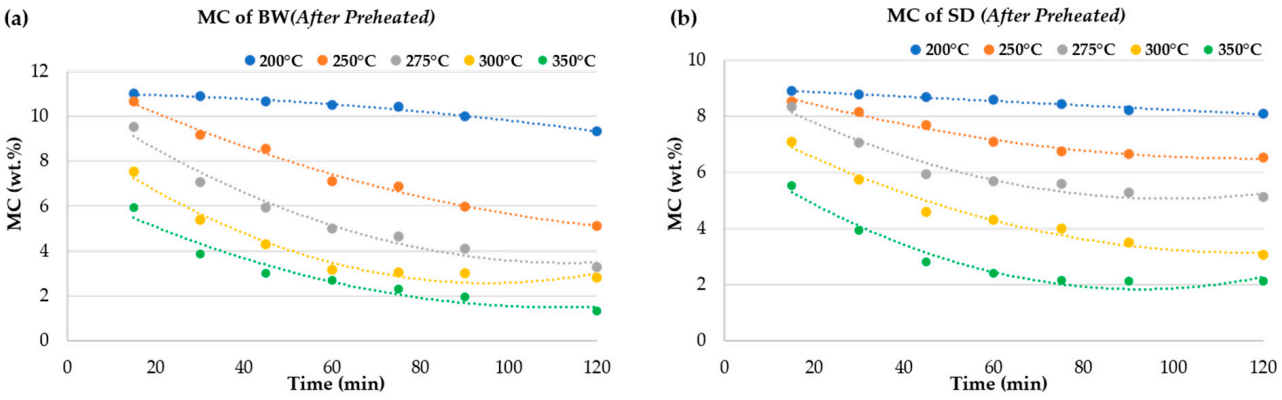


Figure 4. Moisture content (wt.%) of the sample after drying at 105 °C for 24 h: (**a**) BW and (**b**) SD.

The FC content increased with an increasing temperature of the torrefaction process, as depicted in Figure 5. This increase in FC content was attributed to the decrease in VM content, along with potential thermochemical alterations in the components of lignocellulose [46]. At the initial stage of torrefaction, a drying period was likely to occur. The heat was transferred to the biomass particle, causing the temperature to rise onward to the interior particle, at which point the free moisture and VM diffused out into the reactor environment until reaching the equilibrium. As the temperature inside the matrix increased, thermochemical reactions were likely to take place at a higher degree of extent, resulting in the formation of gaseous VM (e.g., light gasses and low MW hydrocarbon compounds) that easily migrated towards the outer layers. Under specific conditions, the majority of the fixed carbon in the biomass is retained while the volatile matter is eliminated [47]. Consequently, with rising temperatures, torrefied samples exhibit higher FC and lower VM contents. High-FC samples generally demonstrate high calorific values, whereas solid fuels with large amounts of VM contents tend to have favorable flammability characteristics, such as ease of ignition. Therefore, torrefaction should be conducted at an optimal temperature to produce a torrefied product that has both HHV and adequate VM content. Compared to coal, biomass typically has higher VM and lower FC contents. For instance, the VM content in coal and biomass generally ranges between 0.9–50 wt.% and 67–88 wt.%, respectively, while the FC content in coal and biomass ranges from 46–92 wt.% to 0.5–20 wt.%, respectively [3].

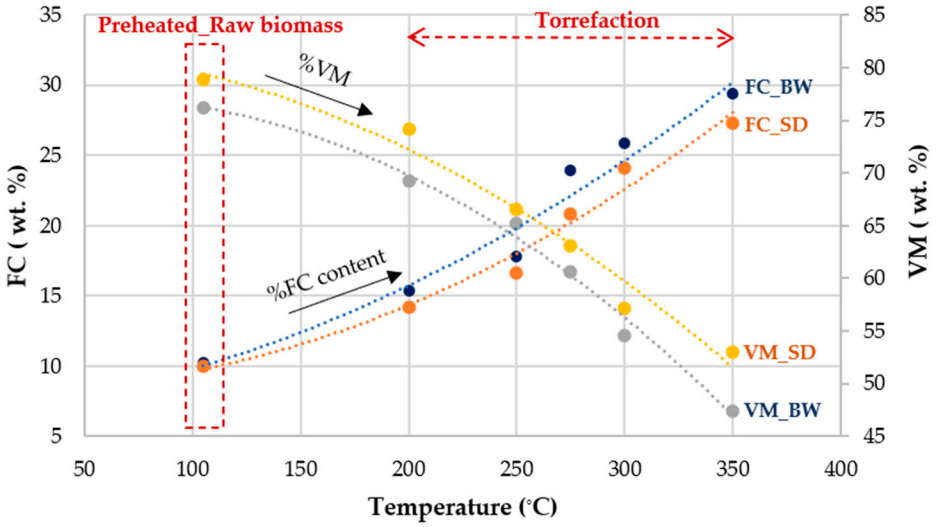


Figure 5. The impact of temperature on the torrefied biomass fixed carbon (%FC) and volatile matter (%VM) content of raw and torrefied BW and SD.

The amount of ash (AC) is regarded as a loss in the process of torrefaction. The amount of ash in the torrefied biomass can vary widely based on the type of biomass and the conditions used during processing, such as temperature and duration of torrefaction [48]. An increase in the torrefaction temperature is likely to cause a linear rise in AC due to the degradation of lignocellulose triggered by thermochemical reactions [49]. From the results, the AC varied from 1.45 wt.% to 20.40 wt.%, as illustrated in Figure 6. With the increasing temperature, BW and SD samples underwent higher degrees of thermal degradation, resulting in greater ash as the end by-product. Under a particular torrefaction temperature, SD tended to yield lower ash content than BW. This is most likely because the SD has more lignin than the BW. The lignin exhibits greater stability in high-temperature environments compared to hemicellulose and cellulose components [50].

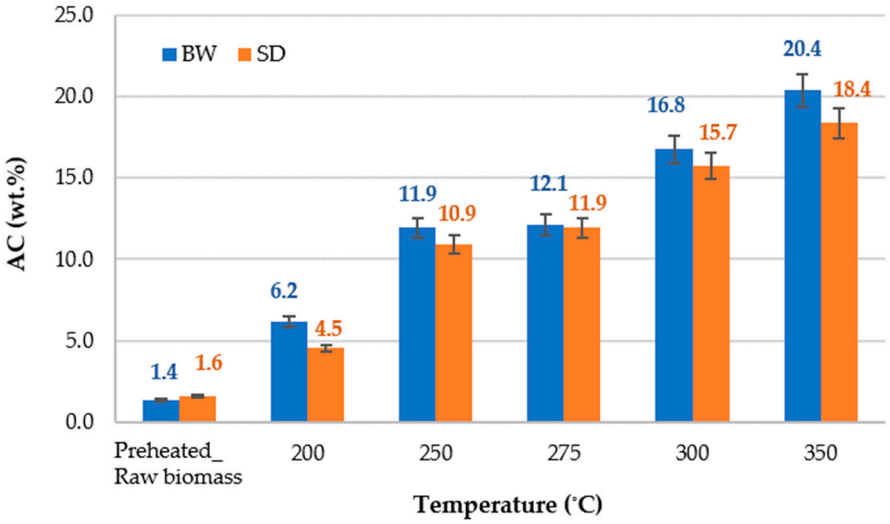


Figure 6. The percentage of AC of the raw and torrefied BW and SD in a range of temperature from 105 °C to 350 °C.

3.2.2. Higher Heating Value (HHV)

Figure 7 illustrates the impact of temperature on the HHV of BW and SD during the torrefaction process. The HHV values (MJ/kg) significantly increased with the increasing torrefaction temperature for both SD and BW, particularly when compared to the base samples being dried at 105 °C. At a given temperature, the torrefied BW samples showed higher HHVs than those of the SD, mainly due to them containing higher FC. For instance, at 105 °C, the HHV of BW is 17.03 MJ/kg, slightly higher than that of SD at 16.89 MJ/kg. This difference becomes more pronounced at higher temperatures, with BW reaching an HHV of 26.09 MJ/kg at 350 °C, compared to SD at 25.1 MJ/kg. The results suggest that BW, under the same torrefaction conditions, generally has a higher HHV than SD, indicating its potential for higher energy yield when subjected to higher temperatures. The HHVs of the raw and torrefied BW and SD from this study were in good agreement with those of various types of fuel as listed in Table 1. The HHVs of all the torrefied samples in this investigation that were processed at a temperature higher than 350 °C exceeded the HHVs of sub-bituminous (25.31 MJ/kg) and bituminous (26.89 MJ/kg) [5].

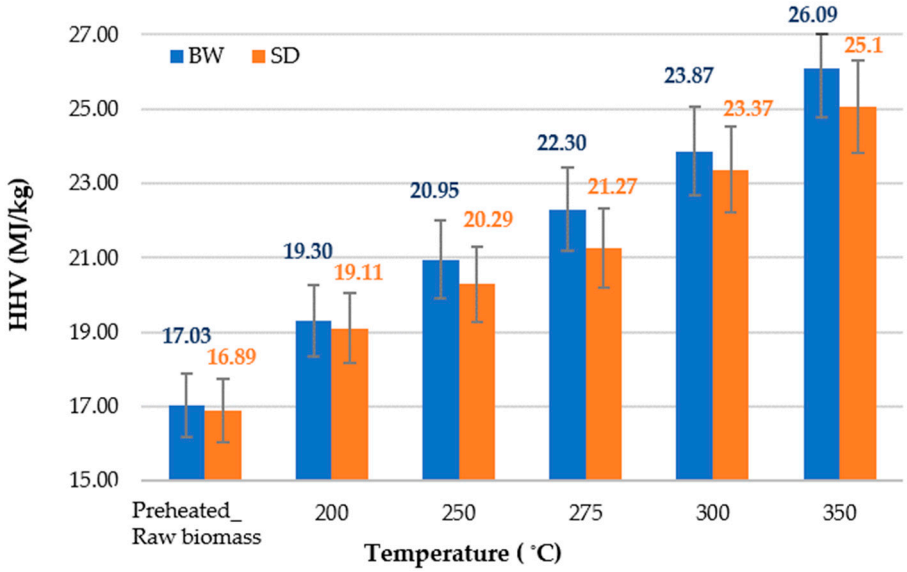


Figure 7. The HHVs of the raw and torrefied BW and SD in a range of temperature from 105 °C to 350 °C.

Table 1. Shows the HHVs (MJ/kg) of a variety of different fuels.

Fuel Type	HHV (MJ/kg)	Reference
Bark wood	17–26	This study
Sawdust	17–25	This study
Palm oil	18–26	[51]
Biogas	20–26	[52,53]
Coal	25–35	[3]
Ethanol	29.7	[54,55]
Biodiesel	37–40	[56]
Crude oil	38–46	[57]
Natural gas	37–55	[58]

3.2.3. Production Yield Analysis

It is possible to assess the torrefied biomass output yield regarding the mass yield of items, which is determined utilizing Equation (2). Figure 8 demonstrates the temperature impact on the total mass yield of the torrefied samples (%). As discussed above, the decomposition of the lignocellulosic compositions within the biomass occurs to a certain extent due to in situ thermochemical reactions [59]. Mass loss inevitably happens, resulting in the formation of small hydrocarbon by-product molecules [60]. The composition change of biomass during torrefaction is also expected to significantly influence the HHV of torrefied materials, which in turn impacts the established E_E (%) values in Equation (3). The temperature increase influences the extent and nature of the components that decompose thermally during torrefaction. A comparison of the total restored HHV is used to determine the EDR of torrefied biomass, and the ratio of the HHV of preheated biomass to the HHV of torrefied biomass, as outlined in Equation (4). Figure 8 further displays the EDR of samples at various torrefaction temperatures. The EDR increases with rising torrefaction temperatures, whereas the mass yield decreases as the temperature increases. From an economic perspective, it is crucial to consider optimal torrefaction temperatures to achieve the desired EDR and high mass yield of torrefied products in large-scale production.

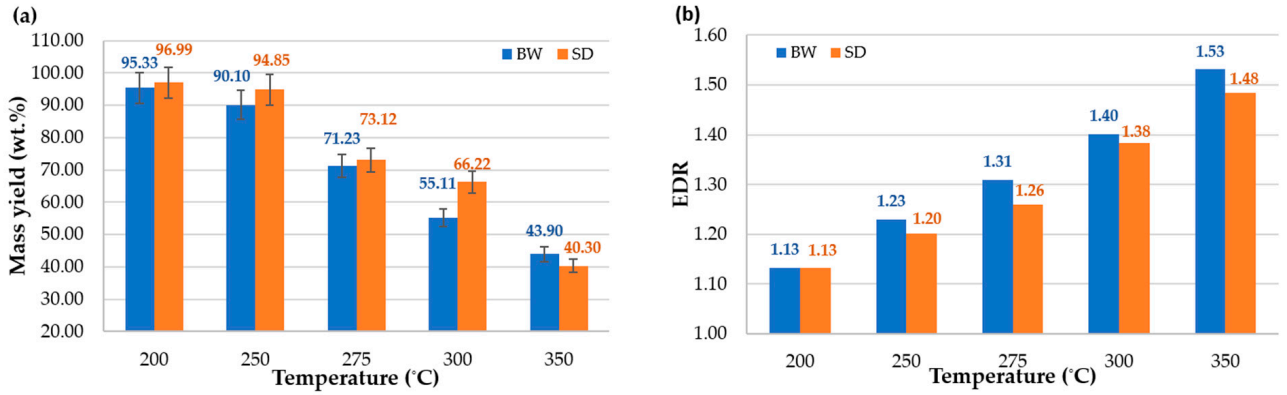


Figure 8. The influence of temperature on the mass yield and EDR of the torrefied BW and SD at 200 °C to 350 °C: (**a**) the mass yield (%), (**b**) EDR.

3.2.4. TGA Results

The thermal degradation associated with the lignocellulose constituents, including cellulose, hemicellulose, and lignin, of the biomass samples was investigated using the TGA analysis, as shown in Figure 9. The weight of both BW and SD samples gradually decreased with increasing temperature, indicating the ongoing decomposition of the materials over the temperature range. The TGA results revealed that the degradation process could occur

in three phases, corresponding to the lignocellulosic compositions. At the earlier stage, the moisture residues were evaporated from the biomass when heating up to about 105 °C, causing a slight reduction in sample weight [61]. The weight progressively decreased with the increasing temperature. At temperatures between 200 °C and 500 °C, the breakdown of hemicellulose, cellulose, and part of the lignin contributed to significant weight reductions. Hemicellulose generally decomposes between 180 °C and 350 °C, while cellulose undergoes rapid degradation between 300 °C and 400 °C [62]. Above 500 °C, major mass loss is likely linked to the continuous breakdown of the lignin constituent which progressively undergoes over a wider temperature region (200 °C to 700 °C) [63]. Two distinctive decomposition temperatures were determined at 295 °C and 345 °C for SD, and 315 °C and 370 °C for BW. Lignin degradation continues even after hemicellulose and cellulose have decomposed, contributing to the slow and extended weight loss at higher temperatures. From the results, it can be interpreted that BW decomposes earlier and more rapidly, while SD displays greater thermal stability, with a more gradual weight loss at higher temperatures. This shift in decomposition behavior reflects the varying contributions of these major biomass constituents across the thermal range.

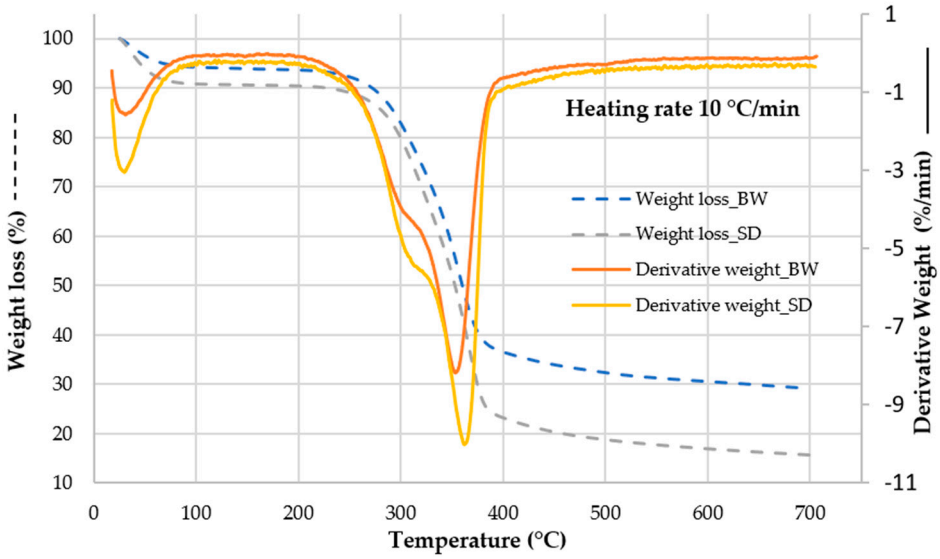


Figure 9. TGA results of the raw BW and SD samples.

3.2.5. Lignocellulose Content Analysis

Long linear polymer cellulose is created when β-glucose molecules polymerize, giving plant cells strength and stiffness in the form of parallel-aligned microfibers bound by hydrogen bonds [64]. Hemicellulose, on the other hand, is a crosslinked polymer based on xylose that connects to lignin and cellulose through interfacial entanglements. [65]. Lignin is a polymer based on phenols that is connected to create inflexible three-dimensional networks that provide strength and decay resistance in plants [66]. Among these components, hemicellulose is generally less stable to thermal treatment compared to cellulose and lignin [65].

Figure 10 demonstrates the effect of torrefaction time and temperature on the shifts in lignocellulose content (i.e., hemicellulose, cellulose, and lignin) of the BW and SD samples. As the temperature rises from 275 °C to 350 °C and the duration extends from 30 min to 120 min, both materials exhibit a significant reduction in weight percentage in hemicellulose and cellulose with increasing lignin content. The amount of hemicellulose in samples that were torrefied and heated to 350 °C significantly reduced by roughly 86% for BW and 78% for SD compared to preheated biomass. Although the reduction was less pronounced, similar trends were observed in the cellulose content. After torrefaction at 350 °C, cellulose contents in BW and SD decreased by about 20% and 36%, respectively. In contrast, all torrefied samples exhibited an increase in lignin content ranging from 50% to 100%, likely

due to the formation of molecules resembling pseudo lignin [67]. In comparison to cellulose and lignin, hemicellulose exhibited the largest percentage drop, suggesting that it was more quickly and more thoroughly thermally degraded into lighter hydrocarbon species. As opposed to hemicellulose, amorphous cellulose degrades more slowly because of its higher degree of polymerization [68]. Because of their shorter chains, hemicelluloses have a lower temperature at which they degrade thermally.

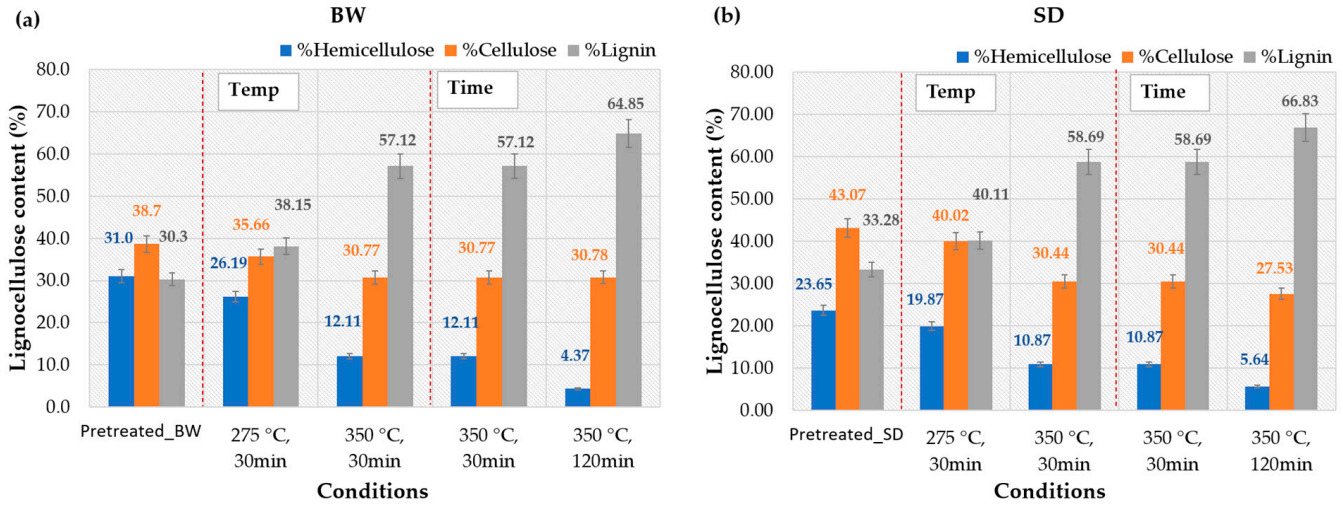


Figure 10. Results from the lignocellulosic analysis of the samples: (**a**) BW and (**b**) SD at various torrefaction temperatures and times.

3.2.6. Analysis Using Fourier Transform Infrared Spectroscopy (FTIR)

Several studies have shown that torrefaction can substantially modify the chemical and physical features of biomass, enhancing its fuel qualities. The biomass changes significantly after torrefaction, mostly as a result of the moisture being removed and changes in the breakdowns caused by thermochemical processes in its chemical structure [31]. FTIR research was performed to look at these modifications. The FTIR spectra of the raw and torrefied biomass for BW and SD are shown in Figure 11, which highlights notable changes following 120 min of torrefaction at 350 °C. The characteristics of the torrefied biomass FTIR spectra give information on alterations in chemical composition that took place throughout the torrefaction. In both materials, there is a notable reduction in the intensity of peaks associated with functional groups indicative of moisture and volatile compounds, such as the broad O–H stretching around 3400 cm^{-1}, which decreases significantly, reflecting the dehydration process during torrefaction [69]. The C–H stretching vibrations were observed around 2930 cm^{-1} and the C=O stretching vibrations between 1600–1850 cm^{-1} also diminished, indicating the breakdown of hemicellulose and cellulose [70]. Comparing BW and SD, the torrefaction of BW shows a more pronounced retention of aromatic structures, as evidenced by the persistent peaks around 1600 cm^{-1}, which are associated with the C=C stretching in lignin [71]. This suggests that BW, compared to SD, retains more of its lignin content after torrefaction, which is consistent with its higher lignin composition. The presence of peaks between 700–900 cm^{-1} in torrefied BW is attributed to C–H bending vibrations in aromatic rings, suggesting that a more stable aromatic structure was achieved in the torrefied BW than in SD. This stability likely contributes to the differences in material properties between the two biomass types after torrefaction.

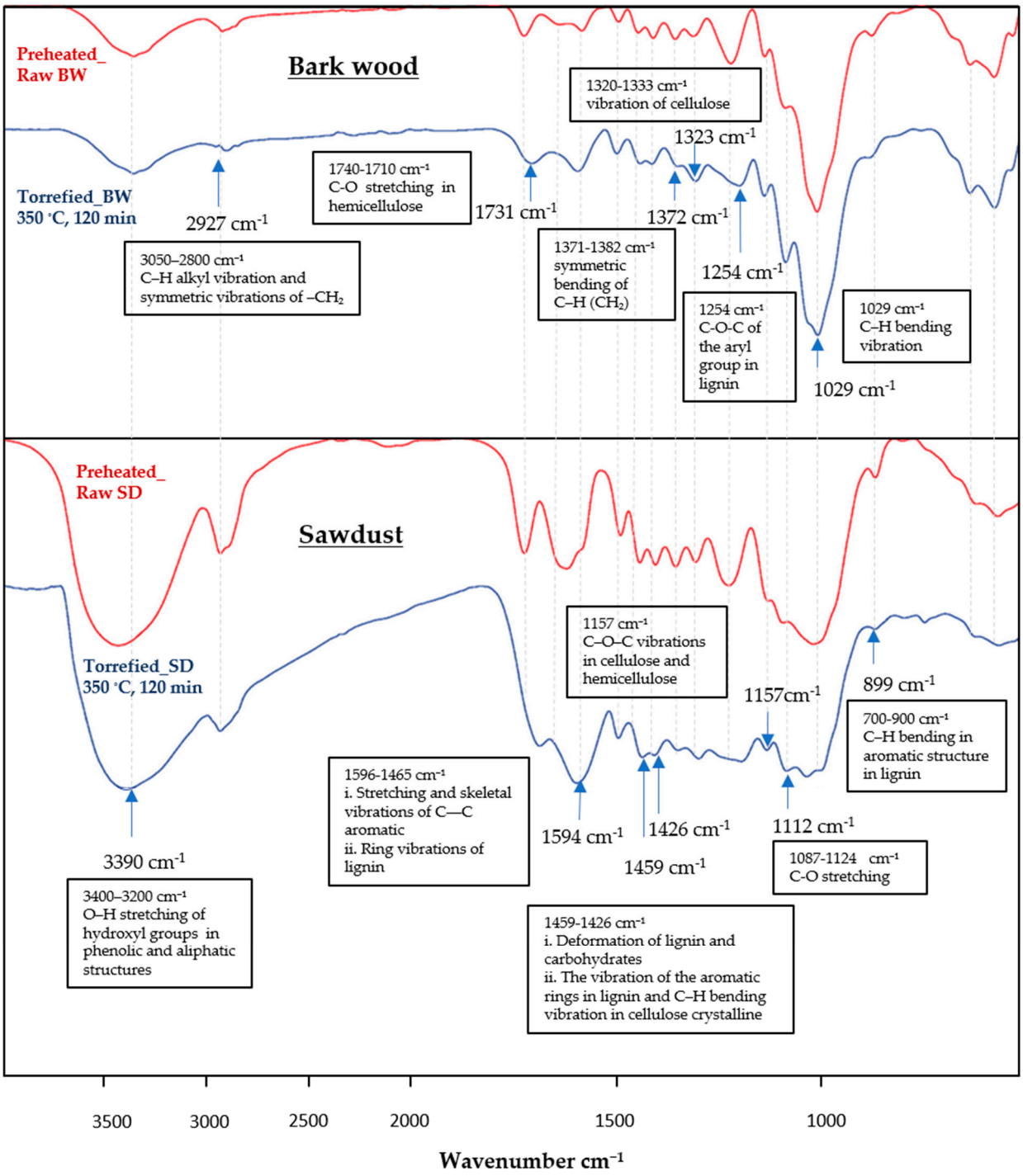


Figure 11. FTIR transmittance spectra of the preheated and torrefied BW and SD at 350 °C, 120 min.

3.2.7. SEM and EDX Analysis

The SEM results provide insight into the surface structure of biomass, revealing changes in the structure and texture as a consequence of the torrefaction process. Figure 12 presents SEM images of BW and SD before and following torrefaction at various temperatures ranging from 200 °C to 350 °C. Post-torrefaction, the micrographs revealed some degree of thermal degradation on the fractured surfaces. The linked cell walls within the porous tubular structure, once with a sharp and well-defined characteristic, were deformed where the presence of collapsed structure was significantly observed.

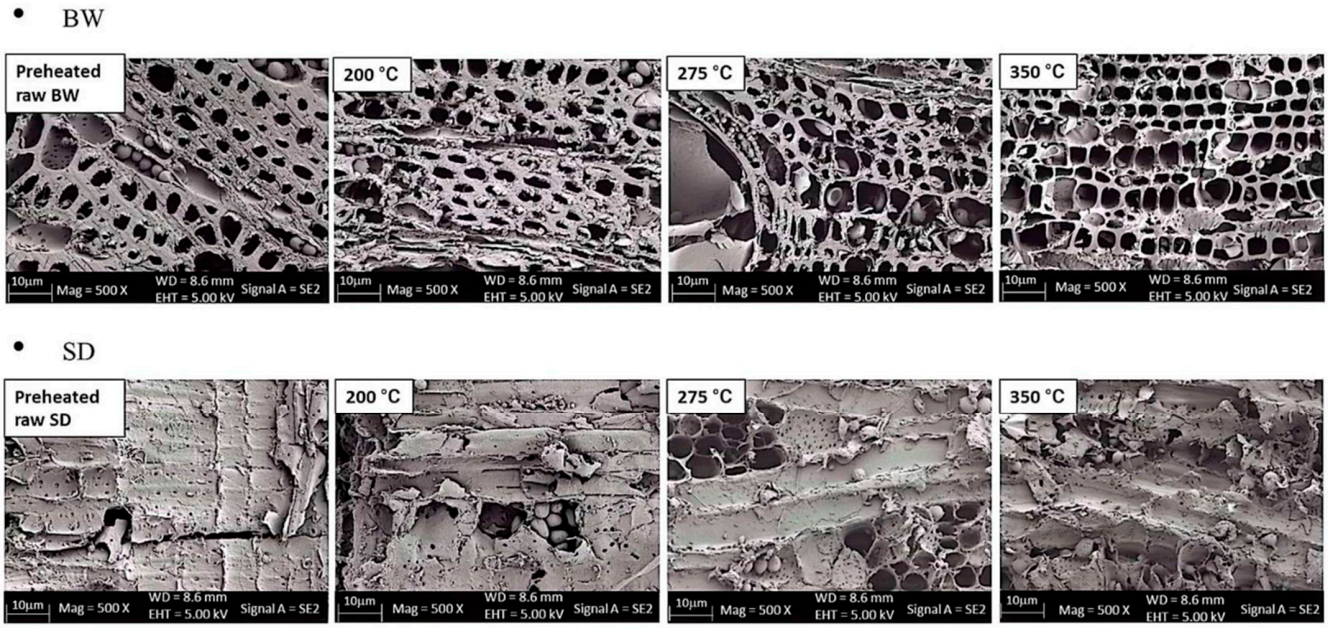


Figure 12. SEM results of the BW and SD samples before (**upper**) and following (**lower**) torrefaction at 200 °C, 275 °C, and 350 °C for 120 min, respectively.

In conjunction with utilizing SEM analysis, the elemental compositions of BW and SD samples were assessed using energy-dispersive X-ray spectroscopy (EDX). The focus was on quantifying the contents of carbon (C) and oxygen (O), the key constituents of the lignocellulose hydrocarbon, expressed by the O/C ratio. Variations in the ratio of O/C values, resulting from the in situ thermochemical processes during torrefaction, significantly influence the biomass fuel qualities [72]. For solid fuel applications, the optimal O/C ratios for torrefied biomass should fall between 0.1 and 0.7, comparable to the values of 0.38 to 0.91 found in fossil coal [38]. The impact of temperature and length of torrefaction on the O/C ratio of atoms of BW and SD samples relative to their original forms is depicted in Figure 13. As was already established, the rate at which lignocellulosic compounds broke down into volatile components was significantly influenced by the torrefaction temperature. Following 120 min of torrefaction at 200 °C, the O/C ratios in the samples decreased by about 14% for BW and 4% for SD. When the temperature reached 350 °C, the O/C ratios dropped significantly by around 67% for BW and 49% for SD, indicating substantial compositional changes due to more extensive thermochemical degradation. The duration of torrefaction also played a role in the extent of degradation, with longer times leading to further reduction in the O/C ratio. At the same torrefaction temperature, the O/C ratio at 350 °C decreased by roughly 55% for BW and 35% for SD as the duration increased from 30 to 120 min. The O/C ratios were in good agreement with the lignocellulose compositions as well as the FTIR results, as discussed earlier.

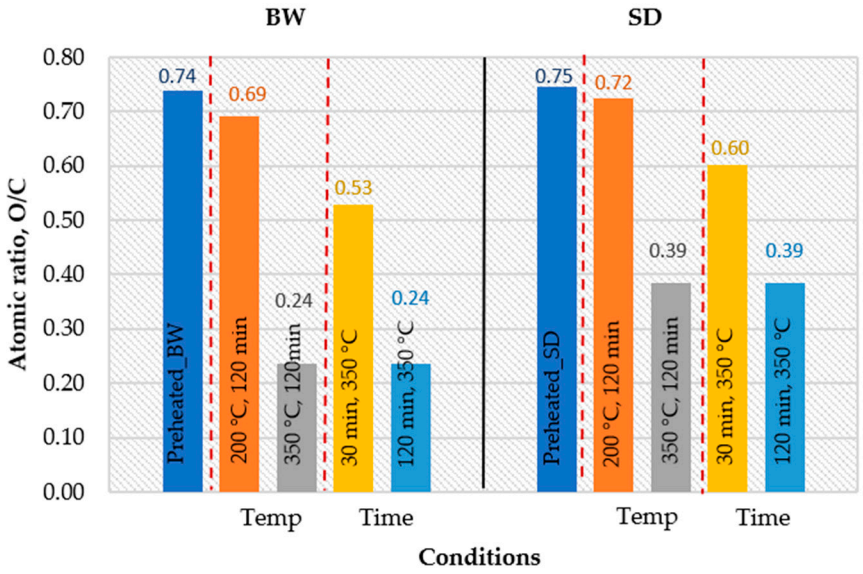


Figure 13. O/C atomic ratio of torrefied SD and BW samples.

3.3. Design Expert Program

3.3.1. Design of Experiments and Analyzing Statistics

Experimental design and RSM responses including HHV, %mass yield, %FC, and eco-efficiency of BW1, BW2, BW3 (preheated BW with diameters of 5 mm, 7.5 mm, and 10 mm, respectively), and SD1, SD2, and SD3 (preheated SD with size of 0.6 mm, 0.85 mm, and 1 mm, respectively), along with the torrefied biomass under various conditions, are listed in Table 2. The impact of three influencing factors—biomass size, torrefaction temperature, and torrefying duration—is shown in Table 2. The projected model equations for BW and SD are represented by Equations (14)–(21), which are obtained by executing the optimization function in the DE to acquire the maximum values of all four responses.

The predicted R^2 of the four responses including HHV, %mass yield, %FC, and eco-efficiency of BW and SD agreed reasonably well with the adjusted R^2. This model can be utilized to explore the design space.

The predicted linear and two-factor interaction (2FI) response equations for HHV, %mass yield, % fixed carbon (FC), and eco-efficiency were derived through multiple regression analysis of the experimental data. These equations, expressed in coded values, are presented as Equations (14)–(21), as seen in Table 3.

The linearity plot of the model ratios of the predicted variables and actual values is shown in Figure 14, demonstrating a significant relationship.

The results confirm the reliability of the suggested model by comparing experimental data with the results from the mathematical model. An efficient method for evaluating models and predicting results is residual analysis, which shows uniformly distributed residuals across absorbed doses and suggests little distortion in the experimental data. Figure 15 displays the simultaneous impacts of three factors on all four responses as well as three-dimensional response surface methodology (RSM) plots and contour plots.

Table 2. Response surface methodology (RSM) applied to the torrefaction process of BW and SD: experimental setup and results.

Run	A: Temp (°C)	B: Time (min)	Bark Wood (BW)					Sawdust (SD)				
			C: Size (mm)	HHV (MJ/kg)	Mass Yield (%)	Fixed Carbon (%)	Eco-Efficiency (kJ/kg CO_{2_eq}*THB)	C: Size (mm)	HHV (MJ/kg)	Mass Yield (%)	Fixed Carbon (%)	Eco-Efficiency (kJ/kg CO_{2_eq}*THB)
BW1/SD1	-	-	5	17.03 ± 0.12		10.28 ± 0.12		0.60	16.88 ± 0.17		9.96 ± 0.25	
BW2/SD2	-	-	7.5	17.00 ± 0.05		10.39 ± 0.09		0.85	16.82 ± 0.10		9.53 ± 0.11	
BW3/SD3	-	-	10	16.91 ± 0.17		10.50 ± 0.11		1.00	16.78 ± 0.23		9.47 ± 0.09	
1	200	30	7.5	18.05 ± 0.25	98.50 ± 1.05	13.30 ± 1.22	31.73	0.85	17.69 ± 0.28	97.97 ± 0.28	10.11 ± 1.01	31.68
2	200	75	5	18.58 ± 0.16	96.83 ± 0.63	14.83 ± 0.21	27.08	0.60	18.15 ± 0.19	97.95 ± 0.13	12.43 ± 0.19	27.80
3	200	75	10	18.42 ± 0.15	97.05 ± 0.41	14.71 ± 0.19	27.25	1.00	18.09 ± 0.19	97.97 ± 0.32	12.32 ± 0.13	27.59
4	200	120	7.5	19.29 ± 0.30	95.33 ± 0.25	15.40 ± 0.28	24.07	0.85	19.10 ± 0.25	96.99 ± 0.24	14.19 ± 0.76	24.21
5	250	30	5	19.13 ± 0.42	96.17 ± 0.13	15.01 ± 0.31	30.74	0.60	18.42 ± 0.38	97.10 ± 0.42	13.67 ± 0.33	31.26
6	250	30	10	19.08 ± 0.18	96.91 ± 0.27	14.89 ± 0.16	30.94	1.00	18.36 ± 0.23	97.37 ± 0.38	13.51 ± 0.42	31.05
7	250	75	7.5	20.21 ± 0.07	94.49 ± 0.03	16.13 ± 0.03	26.71	0.85	18.98 ± 0.02	96.78 ± 0.42	15.93 ± 0.15	26.09
8	250	75	7.5	20.10 ± 0.04	94.37 ± 0.11	15.98 ± 0.18	26.77	0.85	19.03 ± 0.03	95.81 ± 0.55	15.97 ± 0.19	26.08
9	250	75	7.5	20.08 ± 0.06	94.41 ± 0.05	16.11 ± 0.05	26.70	0.85	19.01 ± 0.01	96.70 ± 0.34	15.10 ± 0.68	26.53
10	250	75	7.5	20.19 ± 0.05	94.43 ± 0.03	16.23 ± 0.07	26.66	0.85	19.00 ± 0.00	95.73 ± 0.63	16.01 ± 0.23	26.04
11	250	75	7.5	20.13 ± 0.01	94.58 ± 0.12	16.33 ± 0.17	26.61	0.85	18.98 ± 0.02	96.77 ± 0.41	15.89 ± 0.11	26.12
12	250	120	5	20.95 ± 0.27	90.10 ± 0.22	17.78 ± 0.11	23.24	0.60	20.29 ± 0.12	94.85 ± 0.12	16.66 ± 0.22	23.47
13	250	120	10	20.84 ± 0.23	92.11 ± 0.19	17.61 ± 0.24	23.38	1.00	19.81 ± 0.28	95.13 ± 0.11	16.42 ± 0.17	23.30
14	275	30	5	20.58 ± 0.37	87.57 ± 1.05	17.81 ± 0.19	28.98	0.60	19.89 ± 0.30	93.10 ± 0.54	16.11 ± 0.34	29.99
15	275	30	10	20.50 ± 0.20	88.43 ± 0.43	17.56 ± 0.22	29.19	1.00	19.86 ± 0.23	93.72 ± 0.48	15.95 ± 0.46	29.71
16	275	75	7.5	21.74 ± 0.01	83.34 ± 0.04	19.96 ± 0.14	25.29	0.85	19.95 ± 0.09	86.68 ± 0.34	18.37 ± 0.03	25.27
17	275	75	7.5	21.80 ± 0.05	83.41 ± 0.03	20.13 ± 0.03	25.24	0.85	20.03 ± 0.01	86.89 ± 0.55	18.28 ± 0.06	25.32
18	275	75	7.5	21.77 ± 0.02	83.87 ± 0.49	20.21 ± 0.11	25.20	0.85	20.08 ± 0.04	85.71 ± 0.63	18.31 ± 0.03	25.32
19	275	75	7.5	21.71 ± 0.04	82.99 ± 0.39	20.17 ± 0.07	25.21	0.85	20.09 ± 0.05	86.73 ± 0.39	18.4 ± 0.06	25.27
20	275	75	7.5	21.71 ± 0.04	83.28 ± 0.10	20.01 ± 0.09	25.27	0.85	20.05 ± 0.06	85.70 ± 0.64	18.36 ± 0.02	25.29

Table 2. *Cont.*

Run	A: Temp (°C)	B: Time (min)	Bark Wood (BW)					Sawdust (SD)				
			C: Size (mm)	HHV (MJ/kg)	Mass Yield (%)	Fixed Carbon (%)	Eco-Efficiency (kJ/kg CO_{2_eq}*THB)	C: Size (mm)	HHV (MJ/kg)	Mass Yield (%)	Fixed Carbon (%)	Eco-Efficiency (kJ/kg CO_{2_eq}*THB)
21	275	120	5	22.30 ± 0.38	71.23 ± 0.27	23.95 ± 1.01	21.34	0.60	21.27 ± 0.19	73.12 ± 0.59	20.83 ± 1.11	22.06
22	275	120	10	22.16 ± 0.26	72.90 ± 0.11	23.88 ± 0.22	21.40	1.00	20.78 ± 0.22	74.88 ± 0.28	20.21 ± 1.02	22.38
23	300	30	7.5	22.09 ± 0.16	73.70 ± 0.32	22.67 ± 0.16	28.13	0.85	20.29 ± 0.11	74.85 ± 0.31	19.78 ± 0.10	28.10
24	300	75	5	23.12 ± 0.19	62.90 ± 1.10	23.90 ± 0.23	24.13	0.60	22.43 ± 0.16	71.81 ± 0.36	21.12 ± 0.24	25.18
25	300	75	10	23.05 ± 0.32	64.65 ± 0.64	23.55 ± 0.10	24.31	1.00	22.34 ± 0.10	72.89 ± 0.10	20.9 ± 0.11	25.07
26	300	120	7.5	23.87 ± 0.40	55.11 ± 0.45	25.84 ± 0.19	21.11	0.85	23.37 ± 0.24	66.22 ± 1.06	23.11 ± 0.09	21.27
27	350	30	7.5	23.99 ± 0.13	57.99 ± 0.29	24.17 ± 0.21	27.47	0.85	23.11 ± 0.28	50.87 ± 1.23	22.49 ± 0.15	28.40
28	350	75	5	25.10 ± 0.21	49.14 ± 0.24	28.11 ± 0.37	23.17	0.60	23.97 ± 0.23	46.85 ± 0.49	24.78 ± 0.22	24.17
29	350	75	10	24.77 ± 0.42	50.78 ± 0.57	27.90 ± 0.15	23.22	1.00	23.86 ± 0.19	47.04 ± 0.90	24.53 ± 0.31	24.07
30	350	120	7.5	26.09 ± 0.28	40.30 ± 0.39	29.36 ± 0.17	20.58	0.85	25.06 ± 0.21	43.90 ± 0.23	27.32 ± 0.29	20.69

Table 3. Equations of HHV, %mass yield, %fixed carbon, and eco-efficiency.

Responses	Types	Factors										Equations
		Intercept	A	B	C	AB	AC	BC	A^2	B^2	C^2	
HHV	BW	12.25	4.67×10^{-3}	0.013	0.415	5.9×10^{-5}	-3.14×10^{-4}	-1.33×10^{-4}	6.7×10^{-5}	-5.6×10^{-5}	−0.02	(14)
	SD	28.69	−0.069	−0.02	−12.75	7.7×10^{-5}	−0.002	−0.01	2.0×10^{-4}	1.81×10^{-4}	8.51	(15)
Mass yield	BW	43.78	0.53	0.19	1.67	-8.60×10^{-4}	0.006	0.002	–0.002	-5.6×10^{-4}	−0.21	(16)
	SD	13.79	0.92	0.08	−11.89	-6.64×10^{-4}	0.007	0.05	−0.002	-2.7×10^{-4}	4.62	(17)
Fixed carbon	BW	15.85	−0.041	−0.025	−1.07	2.35×10^{-4}	-1.97×10^{-4}	1.44×10^{-4}	2.12×10^{-4}	3.5×10^{-5}	0.072	(18)
	SD	−8.12	0.05	−0.020	18.60	2.57×10^{-4}	−0.001	−0.012	2.1×10^{-5}	5.2×10^{-5}	11.48	(19)
Eco-efficiency	BW	44.28	−0.056	−0.141	0.29	6.2×10^{-5}	-1.01×10^{-4}	-1.38×10^{-4}	4.0×10^{-5}	2.81×10^{-4}	−0.016	(20)
	SD	55.12	−0.064	−0.140	−23.35	8.98×10^{-6}	0.003	−0.011	6.6×10^{-5}	2.92×10^{-4}	13.38	(21)

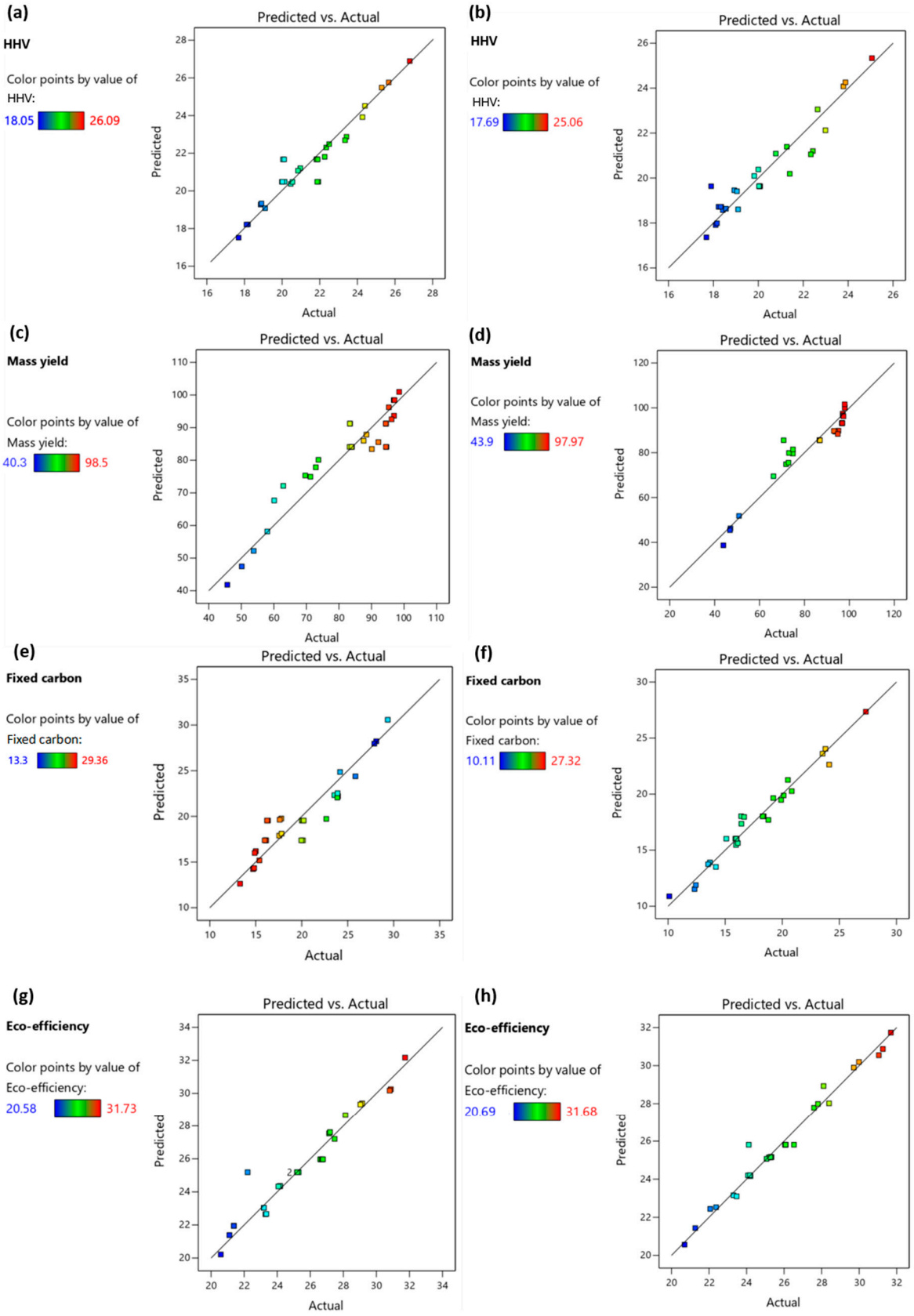


Figure 14. The correlation between actual experimental values and predicted values for HHV (**a**,**b**), %mass yield (**c**,**d**), % fixed carbon (**e**,**f**), and eco-efficiency (**g**,**h**) for BW and SD, respectively.

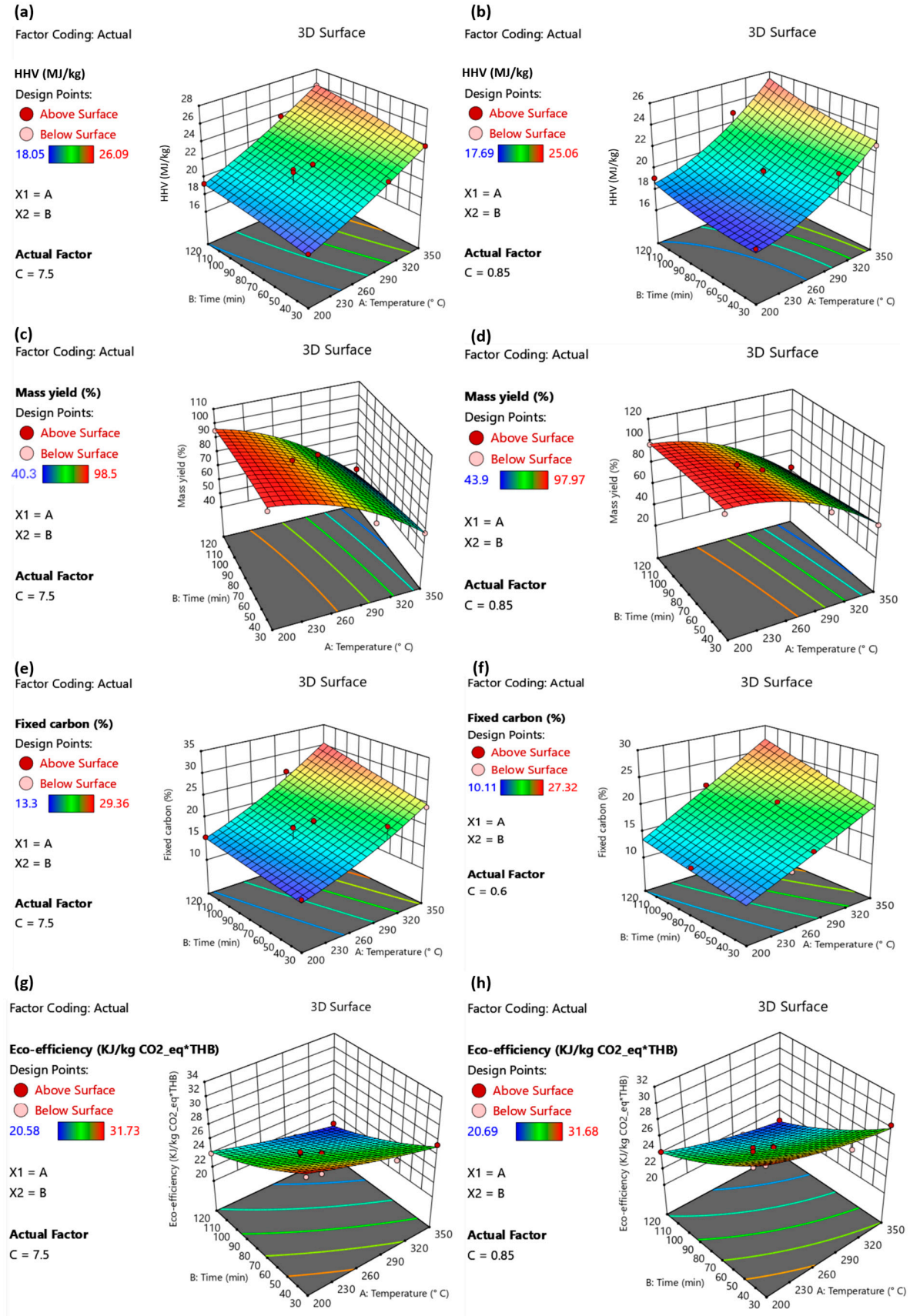


Figure 15. Plots for various parameters using 3D response surface methodology (RSM) plots and contour plots for HHV (**a**,**b**), %mass yield (**c**,**d**), % fixed carbon (**e**,**f**), and eco-efficiency (**g**,**h**) for BW and SD, respectively, during the torrefaction process.

ANOVA analysis of variance was conducted on the model equations, encompassing the coefficient of determination (R^2), adjusted R^2 values, and lack of fit values, to assess the connection and efficacy within the mathematical model. From the results, the ANOVA analysis of HHV yielded model F values of 26.25 and 21.50 for BW and SD, respectively, indicating significant model validity. *p* values below 0.0500 denote significant model terms. In this case, for BW, A (torrefaction temperature) and B (torrefaction time) are identified as significant model terms, whereas for SD, A, B, and A^2 A are significant. The lack-of-fit F-values of 0.27 and 1.42 for BW and SD, respectively, demonstrate that the lack of fit is not significant concerning pure error. The coefficients of determination (R^2), adjusted R^2, and predicted R^2 were calculated as 0.92, 0.91, and 0.89 for BW, and 0.86, 0.89, and 0.81 for SD, respectively. These values further substantiate the robustness and predictive capacity of the models.

For mass yield, the model F-values were 18.72 and 31.33 for BW and SD, respectively, indicating that the model is significant. *p* values less than 0.05 indicate model terms are significant. For mass yield, A, B, and A^2 are significant model terms. The lack of fit F value of 1.14 and 1.23 of BW and SD, respectively, implies the lack of fit is not significant relative to the pure error. R^2 values of 0.89 and 0.93, adjusted R^2 values of 0.84 and 0.90, and predicted R^2 values of 0.79 and 0.84 for BW and SD were reported, respectively.

The statistical analysis for %FC suggested the model F-value of 15.26 and 66.37 of BW and SD, respectively, implying that the model is significant. *p* values less than 0.05 indicate model terms are significant as well. In this case, A and B are significant model terms for BW, while A, B, and AB are significant model factors for SD. The lack of fit F-value of 0.71 and 1.92 of BW and SD, respectively, implies the lack of fit is not significant relative to the pure error. The coefficients R^2, adjusted $R^{2,}$ and predicted R^2 of 0.87, 0.82, and 0.76 were reported for B, and 0.96, 0.95, and 0.91 for SD, respectively.

The statistical analysis of the eco-efficiency model yielded significant F-values of 35.57 and 96.45 for BW and SD, respectively, confirming the validity of the model. Significance is indicated by *p* values below 0.05 for model terms. In the case of BW, factors A and B demonstrated significance, while for SD, factors A, B, B^2, and C^2 (biomass size) were identified as influential. The lack of fit F-values, 0.71 for BW and 0.35 for SD indicates that the lack of fit is not significant relative to pure error. The robustness of the model is further supported by the high coefficients of determination (R^2) values: 0.94 and 0.98 for BW and SD, respectively. Additionally, the adjusted R^2 values of 0.91 and 0.97, along with the predicted R^2 values of 0.90 and 0.96, were reported for BW and SD, respectively.

3.3.2. Confirmation of Conditional Optimizations

The model equations that were utilized to forecast the response values were validated by subjecting them to determine the ideal conditions for torrefaction. The CCD accuracy of the model of the predicted HHV, mass yield, and fixed carbon values was validated by the correlation between the experimental and predicted values. Four levels of torrefaction conditions were examined in the study: an optimal condition established by the prediction software, a lower level (−1), an upper level (+1), and a center level (0). These parameters were used to reassess the dependability of the model in various contexts.

As shown in Table 4, the experiments were repeated with each of the four activation conditions. By comparing the model predictions with the actual experimental data, this repeat was intended to validate the predictions provided by the model. The percentage of error was used to gauge how accurate the predictions of the model were. When comparing the anticipated values to the experimental values, the text notes that the %E values fell between 0.9 and 1.0 percent.

Table 4. Confirmation of conditional optimizations.

Bark Wood (BW)															
Run	**Conditions**			**Predicted**				**Experiment**				**Percentage of Error (%E)**			
	A: Temp (°C)	**B: Time (min)**	**C: Size (mm)**	**HHV (MJ/kg)**	**Mass Yield (%)**	**Fixed Carbon (%)**	**Eco-Efficiency (kJ/kg CO_{2_eq}*THB)**	**HHV (MJ/kg)**	**Mass Yield (%)**	**Fixed Carbon (%)**	**Eco-Efficiency (kJ/kg CO_{2_eq}*THB)**	**HHV**	**Mass Yield**	**Fixed Carbon**	**Eco-Efficiency**
1	350	120	7.5	26.20	41.80	30.58	20.24	25.99 ± 0.22	43.86 ± 0.23	29.38 ± 0.10	20.59	0.99	1.03	0.96	1.01
2	350	75	5	25.20	47.43	28.22	23.07	25.02 ± 0.18	48.82 ± 0.10	27.54 ± 0.16	23.17	0.99	1.03	0.98	1.00
3	350	75	10	24.96	52.20	27.96	23.07	24.83 ± 0.21	49.54 ± 0.16	26.32 ± 0.17	23.22	0.99	0.95	0.94	1.01
4	275	120	5.0	22.29	74.92	22.21	21.95	22.25 ± 0.11	73.30 ± 0.11	22.00 ± 0.28	21.34	1.00	0.98	0.99	0.97
5	275	30	5.0	20.48	85.98	18.10	29.35	20.36 ± 0.29	83.11 ± 0.19	17.87 ± 0.19	28.98	0.99	0.97	0.99	0.99
6	200	120	7.5	19.26	96.21	15.18	24.33	19.25 ± 0.33	95.67 ± 0.21	15.13 ± 0.20	24.07	1.00	0.99	1.00	0.99
Sawdust (SD)															
Run	**Conditions**			**Predicted**				**Experiment**				**Percentage of Error (%E)**			
	A: Temp (°C)	**B: Time (min)**	**C: Size (mm)**	**HHV (MJ/kg)**	**Mass Yield (%)**	**Fixed Carbon (%)**	**Eco-Efficiency (kJ/kg CO_{2_eq}*THB)**	**HHV (MJ/kg)**	**Mass Yield (%)**	**Fixed Carbon (%)**	**Eco-Efficiency (kJ/kg CO_{2_eq}*THB)**	**HHV**	**Mass Yield**	**Fixed Carbon**	**Eco-Efficiency**
1	350	120	0.85	25.32	38.68	27.32	20.56	24.95 ± 0.19	49.87 ± 0.20	26.66 ± 0.11	20.07	0.99	1.29	0.98	0.98
2	350	75	0.60	24.24	45.42	24.01	24.21	23.95 ± 0.25	46.15 ± 0.16	23.77 ± 0.24	24.17	0.99	1.02	0.99	1.00
3	350	75	1.00	24.06	46.25	23.59	24.20	23.85 ± 0.32	39.99 ± 0.31	23.10 ± 0.16	24.07	0.99	0.86	0.98	0.99
4	275	120	0.60	21.39	79.89	20.25	22.44	21.21 ± 0.17	78.85 ± 0.22	18.48 ± 0.26	22.26	0.99	0.99	0.91	0.99
5	275	30	0.60	19.40	89.71	15.62	30.19	19.01 ± 0.22	89.93 ± 0.25	14.61 ± 0.18	29.99	0.98	1.00	0.94	0.99
6	200	120	0.85	18.62	97.43	13.50	24.16	17.70 ± 0.29	97.56 ± 0.63	13.38 ± 0.08	24.21	0.95	1.00	0.99	1.00

3.3.3. Optimal Condition and Validation

To optimize the trade-off between higher heating value (HHV) and mass yield in relation to torrefaction time and temperature [73], a differential evolution (DE) optimizer function was implemented. This approach enabled the simultaneous determination of optimal conditions for both response variables, ensuring a balanced and efficient torrefaction process. The utilization of such advanced optimization techniques is crucial for maximizing the effectiveness of biomass pre-treatment methods in the renewable energy sector. The response optimizer tool in the statistical program was used to investigate the best conditions for producing torrefied biomass. The optimal conditions for generating high-quality torrefied BW were achieved at a temperature of 325 °C, torrefaction time of 30 min, and biomass size of 8.5 mm, since these conditions achieved the maximum values of HHV (22.72 MJ/kg), %mass yield (70.39 wt.%), %FC content (22.23 wt.%), and eco-efficiency (27.89 MJ/THB) simultaneously, as shown in Figure 16a. The optimal conditions of the torrefaction process for SD were at 320 °C, with a torrefaction duration of 30 min, and biomass size of 0.60 mm, resulting in an HHV of 21.53 MJ/kg, %mass yield of 70.16 wt.%, %FC content of 18.80 wt.%, and eco-efficiency of 29.18 MJ/THB, as illustrated in Figure 16b.

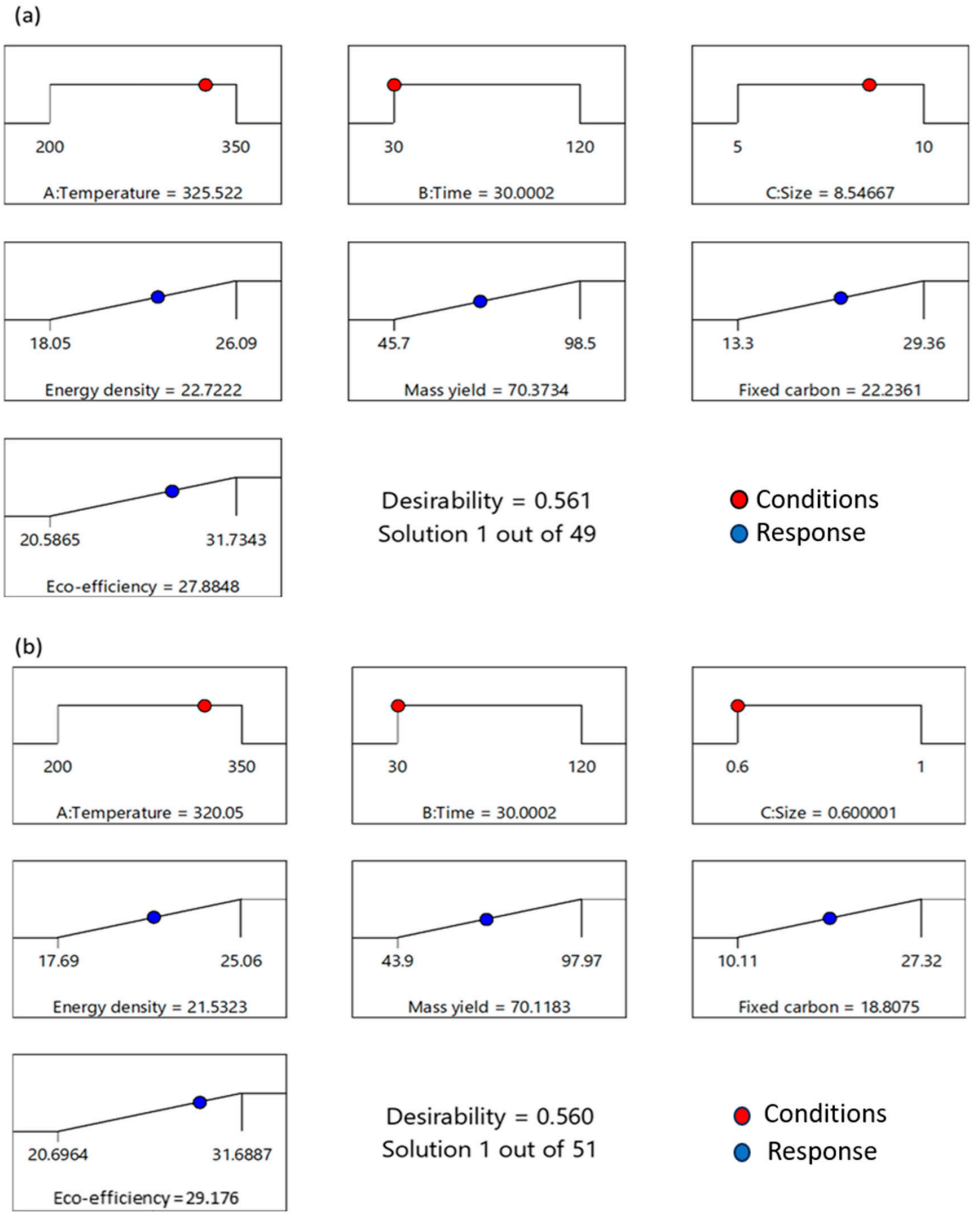


Figure 16. Desirability ramps of optimal conditions for (**a**) BW and (**b**) SD.

3.4. CO_2 Equivalent Estimation

Figure 17 illustrates the relationship between the temperature (°C) and CO_{2_eq} values (kg CO_2/kg biomass) for torrefied biomass, comparing BW and SD. As the temperature increases from 105 °C to 350°C, the CO_2 equivalent values for both materials rise. Initially, at lower temperatures (105 °C to 200 °C), the CO_2 values for BW and SD are relatively low and similar, with BW having slightly lower values. However, as the temperature increases to higher levels (250 °C to 350 °C), the CO_2 values significantly increase, with BW generally exhibiting higher CO_2 equivalent values than SD, particularly at the highest temperature of 350 °C. This suggests that higher torrefaction temperatures lead to greater CO_2 emissions for both types of biomass, with BW contributing slightly more to CO_2 emissions than SD. In comparison, the CO_{2_eq} emissions are similar, ranging from 0.75 to 1.35 kg CO_{2_eq}/kg for plywood. This range aligns well with the CO_{2_eq} emissions reported for torrefied biomass production, indicating a good agreement.

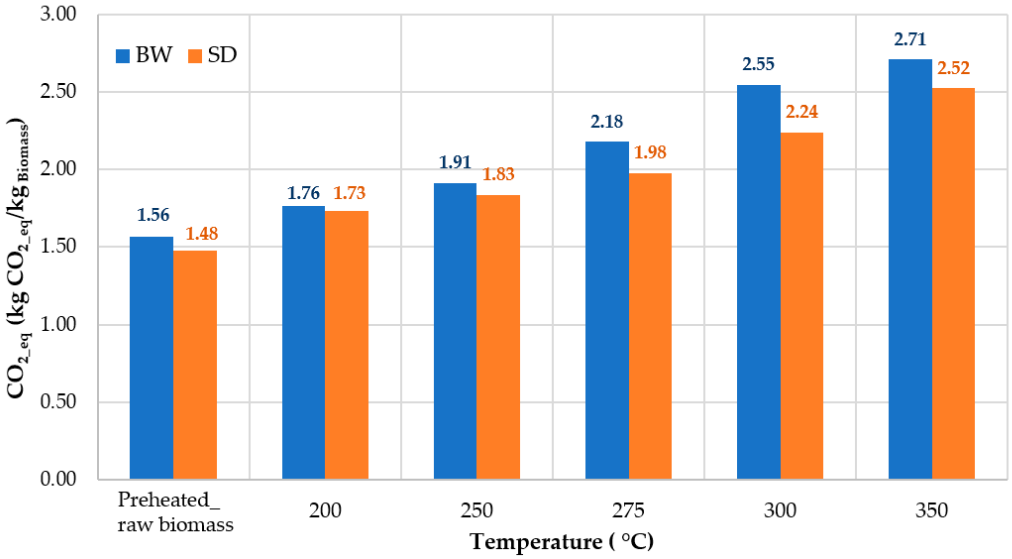


Figure 17. Influence of temperature on CO_2 equivalent emission values of the torrefied BW and SD.

3.5. Eco-Efficiency

Figure 18 demonstrates the relation between the circumstances of torrefaction and the eco-efficiency of torrefied biomass. Values for eco-efficiency decreased with increasing torrefaction temperature and time. It was discovered that while particle size has little bearing on the efficiency value, torrefaction temperature and time are important model parameters. Since fixed and operating expenses are the basis for determining eco-efficiency, it was found that eco-efficiency declines with the length of the torrefaction time. As seen in Figure 18, the highest eco-efficiency of torrefied BW and SD was approximately 31.74 and 31.69 kJ/kg CO_{2_eq}*THB), obtained from the torrefaction process at 200 °C and 30 min.

A comparative analysis of the eco-efficiency properties between torrefied biomass and coal was conducted. To estimate the eco-efficiency of coal, the coal composition comprises 52% bituminous coal and 17% lignite by weight used in the calculation [74]. This specific composition is utilized in determining the HHV of coal, which has been calculated to be 19.53 MJ/kg. Regarding CO_2 emissions from coal combustion, it is estimated that bituminous coal produces 0.0915 kg CO_{2_eq}/MJ, while lignite emits 0.0943 kg CO_{2_eq}/MJ [75] when burned in a bone-dry state. These values correspond to CS of 2.57 kg CO_{2_eq}/kg coal and CBB of 1.80 kg CO_{2_eq}/kg coal, respectively. Current market analysis indicates that the price of coal is 4.02 THB/kg [76]. Utilizing the optimal condition derived from the DE program, as depicted in Figure 16, the eco-efficiency of coal combustion has been determined to be 13.72 kJ/(kg CO_{2_eq}*THB), based on the application of Equation (13), revealing enhanced characteristics in the former.

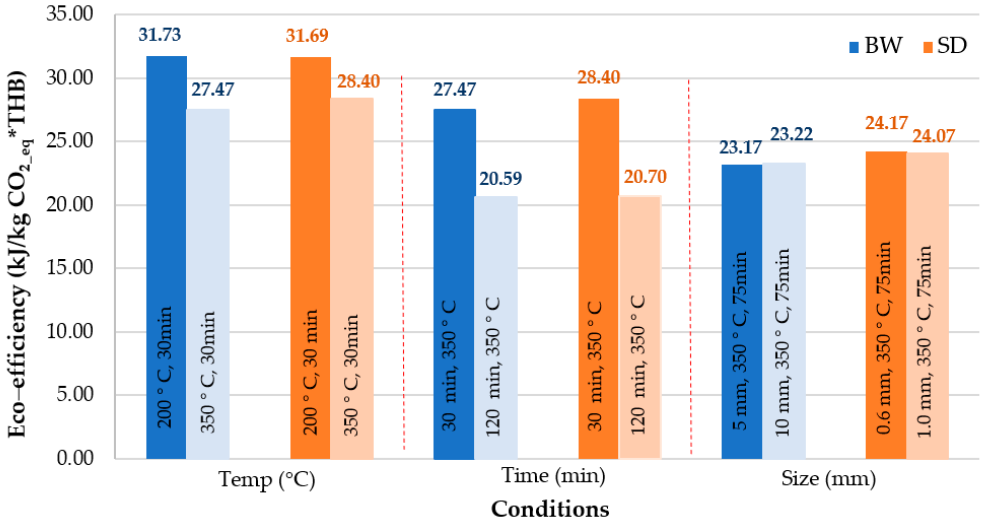


Figure 18. Effects of time, temperature, and particle size on torrefied biomass eco-efficiency values.

4. Conclusions

The results demonstrate that increasing torrefaction temperature and duration significantly improves the HHV of torrefied biomass, reaching 17–26 MJ/kg, comparable to that of sub-bituminous coal. Torrefaction at 300 °C for 30 min represents an optimal processing window, yielding biomass with properties comparable to sub-bituminous coal while maximizing eco-efficiency when considered from a life cycle analysis (LCA) perspective. The findings position torrefied biomass as a technically viable and environmentally conscious alternative to fossil fuels. This research provides a foundational framework for scaling torrefaction technology, particularly in regions with abundant biomass resources. Future investigations should focus on process optimization at industrial scales and comprehensive techno-economic analyses to facilitate widespread adoption in commercial power generation applications. These findings contribute significantly to the ongoing transition toward sustainable energy systems while maintaining the high energy density requirements of modern industrial processes.

Author Contributions: A.K. and W.D.: conceptualized and supervised the study, designed methodology and validated the experiments, interpreted the data, and contributed to the writing, reviewing, and editing of the manuscript; J.K.: performed the experiments, analyzed and illustrated the experimental results, drafted the original manuscript, and wrote, reviewed, and edited the manuscript. All authors have read and agreed to the published version of the manuscript.

Funding: This research was funded by The Ph.D. Excellence Scholarship, Walailak University, Contract No. 18/2022.

Data Availability Statement: The results presented in this study along with data and code supporting the findings from this study are available upon further request to the corresponding author.

Acknowledgments: The authors extend their sincere appreciation to Walailak University for providing laboratory support. We are also deeply grateful to Khaomahachai Parawood Co., Ltd. for generously supplying the biomass raw materials used in this study. The authors declare the use of AI tools, including Grammarly and QuillBot for grammar and language editing assistance, as well as Turnitin for checking similarity and plagiarism.

Conflicts of Interest: The authors confirm that there are no conflicts of interest associated with this study.

Nomenclature

%C	Cellulose content
%E	Acetone extractable content
%H	Hemicellulose content
%L	Lignin content
AC	Ash content
BW	Bark wood
CBB	CO2 of torrefied biomass
CC	Carbon content
CO_{2_eq}	Total CO_2 equivalent
CS	Carbon storage
DE	Design Expert
EDX	Energy-dispersive X-ray spectroscopy
EDR	Energy densification ratio
E_E	Energy efficiency
FC	Fixed carbon
FTIR	Fourier transform infrared
HHV	Higher heating value
MC	Moisture content
SD	Sawdust
SEM	Scanning electron microscopy
TGA	Thermogravimetric analysis
VM	Volatile matters
Y_M	Mass yield

References

1. Höök, M.; Tang, X. Depletion of fossil fuels and anthropogenic climate change—A review. *Energy Policy* **2013**, *52*, 797–809. [CrossRef]
2. Holechek, J.L.; Geli, H.M.E.; Sawalhah, M.N.; Valdez, R. A Global Assessment: Can Renewable Energy Replace Fossil Fuels by 2050? *Sustainability* **2022**, *14*, 4792. [CrossRef]
3. Chen, W.-H.; Lin, B.-J.; Lin, Y.-Y.; Chu, Y.-S.; Ubando, A.T.; Show, P.L.; Ong, H.C.; Chang, J.-S.; Ho, S.-H.; Culaba, A.B.; et al. Progress in biomass torrefaction: Principles, applications and challenges. *Prog. Energy Combust. Sci.* **2021**, *82*, 100887. [CrossRef]
4. Liang, W.; Jiang, C.; Wang, G.; Ning, X.; Zhang, J.; Guo, X.; Xu, R.; Wang, P.; Ye, L.; Li, J.; et al. Research on the co-combustion characteristics and kinetics of agricultural waste hydrochar and anthracite. *Renew. Energy* **2022**, *194*, 1119–1130. [CrossRef]
5. Mohamad, N.F.; Hidayu, A.R.; Sherif, A.A.; Sharifah, A.S.A.K. Characteristics of bituminous coal, sub-bituminous coal and bottom ash from a coal-fired power plant. In Proceedings of the BEIAC 2013—2013 IEEE Business Engineering and Industrial Applications Colloquium, Langkawi, Malaysia, 7–9 April 2013; pp. 571–573.
6. Liu, Z.; Quek, A.; Hoekman, S.K.; Srinivasan, M.; Balasubramanian, R. Thermogravimetric investigation of hydrochar-lignite co-combustion. *Bioresour. Technol.* **2012**, *123*, 646–652. [CrossRef]
7. Yoro, K.O.; Daramola, M.O. CO_2 emission sources, greenhouse gases, and the global warming effect. In *Advances in Carbon Capture*; Woodhead Publishing: Sawston, UK, 2020; pp. 3–28. [CrossRef]
8. Esteves, B.; Sen, U.; Pereira, H. Influence of Chemical Composition on Heating Value of Biomass: A Review and Bibliometric Analysis. *Energies* **2023**, *16*, 4226. [CrossRef]
9. Kota, K.B.; Shenbagaraj, S.; Sharma, P.K.; Sharma, A.K.; Ghodke, P.K.; Chen, W.-H. Biomass torrefaction: An overview of process and technology assessment based on global readiness level. *Fuel* **2022**, *324*, 124663. [CrossRef]
10. Sher, F.; Yaqoob, A.; Saeed, F.; Zhang, S.; Jahan, Z.; Klemeš, J.J. Torrefied biomass fuels as a renewable alternative to coal in co-firing for power generation. *Energy* **2020**, *209*, 118444. [CrossRef]
11. Liu, Y.; Tan, W.; Liang, S.; Bi, X.; Sun, R.; Pan, X. Comparative study on the co-combustion behavior of torrefied biomass blended with different rank coals. *Biomass Convers. Biorefinery* **2022**, *14*, 781–793. [CrossRef]
12. Thanapal, S.S.; Annamalai, K.; Ansley, R.J.; Ranjan, D. Co-firing carbon dioxide-torrefied woody biomass with coal on emission characteristics. *Biomass Convers. Biorefinery* **2016**, *6*, 91–104. [CrossRef]
13. Olugbade, T.O.; Ojo, O.T. Biomass Torrefaction for the Production of High-Grade Solid Biofuels: A Review. *BioEnergy Res.* **2020**, *13*, 999–1015. [CrossRef]
14. Wild, M.; Calderón, C. Torrefied Biomass and Where Is the Sector Currently Standing in Terms of Research, Technology Development, and Implementation. *Front. Energy Res.* **2021**, *9*, 678492. [CrossRef]
15. Proskurina, S.; Heinimö, J.; Schipfer, F.; Vakkilainen, E. Biomass for industrial applications: The role of torrefaction. *Renew. Energy* **2017**, *111*, 265–274. [CrossRef]

16. Nunes, L.; Matias, J.; Catalão, J. A review on torrefied biomass pellets as a sustainable alternative to coal in power generation. *Renew. Sustain. Energy Rev.* **2014**, *40*, 153–160. [CrossRef]
17. Lee, Y.; Yang, W.; Chae, T.; Kang, B.; Park, J.; Ryu, C. Comparative Characterization of a Torrefied Wood Pellet under Steam and Nitrogen Atmospheres. *Energy Fuels* **2018**, *32*, 5109–5114. [CrossRef]
18. Leepromrath, S.; Zhou, J.; Zhou, D. The impacts of crop diversity adoption on Rubber Farmers' Welfare: Evidence from Thailand. *Agrofor. Syst.* **2024**, *98*, 1377–1397. [CrossRef]
19. Kongto, P.; Palamanit, A.; Chaiprapat, S.; Tippayawong, N.; Khempila, J.; Ruangim, P. Key fuel characteristics and techno-economic aspects of torrefied rubberwood biomass pellets produced by incorporating various cassava-based binders at varied doses. *Environ. Sci. Pollut. Res.* **2024**, *31*, 37663–37680. [CrossRef]
20. Kongto, P.; Palamanit, A.; Chaiprapat, S.; Tippayawong, N. Enhancing the fuel properties of rubberwood biomass by moving bed torrefaction process for further applications. *Renew. Energy* **2021**, *170*, 703–713. [CrossRef]
21. Leepromrath, S.; Zhu, J.; Zhou, J.; Li, T.; Zhou, D. Rubber crop diversity and its influential factors in Thailand. *J. Rubber Res.* **2021**, *24*, 461–473. [CrossRef]
22. Murphy, D.J.; Goggin, K.; Paterson, R.R.M. Oil palm in the 2020s and beyond: Challenges and solutions. *CABI Agric. Biosci.* **2021**, *2*, 39. [CrossRef]
23. Chittella, H.; Yoon, L.W.; Ramarad, S.; Lai, Z.-W. Rubber waste management: A review on methods, mechanism, and prospects. *Polym. Degrad. Stab.* **2021**, *194*, 109761. [CrossRef]
24. Indexmundi, Wood Pulp Monthly Price. 2024. Available online: https://www.indexmundi.com/commodities/?commodity=wood-pulp&months=120%C2%A4cy=thb (accessed on 18 September 2024).
25. Sarker, T.R.; Nanda, S.; Dalai, A.K.; Meda, V. A Review of Torrefaction Technology for Upgrading Lignocellulosic Biomass to Solid Biofuels. *BioEnergy Res.* **2021**, *14*, 645–669. [CrossRef]
26. Chen, D.; Cen, K.; Zhuang, X.; Gan, Z.; Zhou, J.; Zhang, Y.; Zhang, H. Insight into biomass pyrolysis mechanism based on cellulose, hemicellulose, and lignin: Evolution of volatiles and kinetics, elucidation of reaction pathways, and characterization of gas, biochar and bio-oil. *Combust. Flame* **2022**, *242*, 112142. [CrossRef]
27. Javanmard, A.; Patah, M.F.A.; Zulhelmi, A.; Daud, W.M.A.W. A comprehensive overview of the continuous torrefaction method: Operational characteristics, applications, and challenges. *J. Energy Inst.* **2023**, *108*, 101199. [CrossRef]
28. Chang, S.; Zhao, Z.; Zheng, A.; He, F.; Huang, Z.; Li, H. Characterization of Products from Torrefaction of Sprucewood and Bagasse in an Auger Reactor. *Energy Fuels* **2012**, *26*, 7009–7017. [CrossRef]
29. Mamvura, T.A. Overview of Torrefaction Technologies: A Path Getaway for Waste-to-Energy. In *Handbook of Waste Biorefinery*; Springer International Publishing: Cham, Switzerland, 2022; pp. 1–25. [CrossRef]
30. Sarker, T.R.; Azargohar, R.; Dalai, A.K.; Venkatesh, M. Physicochemical and Fuel Characteristics of Torrefied Agricultural Residues for Sustainable Fuel Production. *Energy Fuels* **2020**, *34*, 14169–14181. [CrossRef]
31. Bach, Q.-V.; Skreiberg, O. Upgrading biomass fuels via wet torrefaction: A review and comparison with dry torrefaction. *Renew. Sustain. Energy Rev.* **2016**, *54*, 665–677. [CrossRef]
32. Olumide Olugbade, T. Economics, Sustainability, and Reaction Kinetics of Biomass Torrefaction. In *Biotechnological Applications of Biomass*; IntechOpen: London, UK, 2021; pp. 1–34. [CrossRef]
33. Sousa, L.M.; Ogura, A.P.; Anchieta, C.G.; Morin, M.; Canabarro, N.I. Biomass Torrefaction for Renewable Energy: From Physicochemical, Bulk Properties, and Flowability to Future Perspectives and Applications. *Energy Fuels* **2024**, *38*, 18367–18385. [CrossRef]
34. Doddapaneni, T.R.K.C.; Praveenkumar, R.; Tolvanen, H.; Rintala, J.; Konttinen, J. Techno-economic evaluation of integrating torrefaction with anaerobic digestion. *Appl. Energy* **2018**, *213*, 272–284. [CrossRef]
35. Abdulyekeen, K.A.; Umar, A.A.; Patah, M.F.A.; Daud, W.M.A.W. Torrefaction of biomass: Production of enhanced solid biofuel from municipal solid waste and other types of biomass. *Renew. Sustain. Energy Rev.* **2021**, *150*, 111436. [CrossRef]
36. *ISO 565:1990*; Test Sieves. International Organization for Standardization: Geneva, Switzerland, 1990. Available online: www.iso.org/obp/ui/#iso:std:iso:565:ed-3:v1:en (accessed on 18 September 2024).
37. ASTM International, ASTM E11.Standard Specification for Woven Wire Test Sieves. 2020. Available online: https://advantechmfg.com/astm-e11-standards-table-and-calculator/ (accessed on 18 September 2024).
38. Aguado, R.; Cuevas, M.; Pérez-Villarejo, L.; Martínez-Cartas, M.L.; Sánchez, S. Upgrading almond-tree pruning as a biofuel via wet torrefaction. *Renew. Energy* **2019**, *145*, 2091–2100. [CrossRef]
39. Sluiter, A.D.; Templeton, D.W. Determination of Structural Carbohydrates and Lignin in Biomass: Laboratory Analytical Procedure (LAP) (Revised July 2011). 2008. Available online: https://www.nrel.gov/docs/gen/fy13/42618.pdf (accessed on 23 October 2024).
40. Niu, Y.; Lv, Y.; Lei, Y.; Liu, S.; Liang, Y.; Wang, D.; Hui, S. Biomass torrefaction: Properties, applications, challenges, and economy. *Renew. Sustain. Energy Rev.* **2019**, *115*, 109395. [CrossRef]
41. Changwichan, K.; Silalertruksa, T.; Gheewala, S.H. Eco-Efficiency Assessment of Bioplastics Production Systems and End-of-Life Options. *Sustainability* **2018**, *10*, 952. [CrossRef]

42. Heilala, J.; Ruusu, R.; Montonen, J.; Vatanen, S.; Kavka, C.; Asnicar, F.; Scholze, S.; Armiojo, A.; Insunza, M. Eco-process Engineering System for Collaborative Product Process System Optimisation. In *Advances in Production Management Systems: Innovative and Knowledge-Based Production Management in a Global-Local World*; Springer: Berlin/Heidelberg, Germany, 2014; pp. 1–12. [CrossRef]
43. Bergman, R.; Puettmann, M.; Taylor, A.; Skog, K.E. The Carbon Impacts of Wood Products. *For. Prod. J.* **2014**, *64*, 220–231. [CrossRef]
44. Mary, S. Booth, Carbon Emissions from Burning Biomass for Energy. 2011. Available online: https://policycommons.net/artifacts/2246921/carbon-emissions-from-burning-biomass-for-energy/ (accessed on 18 September 2024).
45. Maksimuk, Y.; Antonava, Z.; Krouk, V.; Korsakova, A.; Kursevich, V. Prediction of higher heating value (HHV) based on the structural composition for biomass. *Fuel* **2021**, *299*, 120860. [CrossRef]
46. Premchand, P.; Demichelis, F.; Chiaramonti, D.; Bensaid, S.; Fino, D. Study on the effects of carbon dioxide atmosphere on the production of biochar derived from slow pyrolysis of organic agro-urban waste. *Waste Manag.* **2023**, *172*, 308–319. [CrossRef]
47. Chen, D.; Zheng, Z.; Fu, K.; Zeng, Z.; Wang, J.; Lu, M. Torrefaction of biomass stalk and its effect on the yield and quality of pyrolysis products. *Fuel* **2015**, *159*, 27–32. [CrossRef]
48. Ribeiro, J.M.C.; Godina, R.; Matias, J.C.d.O.; Nunes, L.J.R. Future Perspectives of Biomass Torrefaction: Review of the Current State-Of-The-Art and Research Development. *Sustainability* **2018**, *10*, 2323. [CrossRef]
49. Mohammad, I.N.; Ongkudon, C.M.; Misson, M. Physicochemical Properties and Lignin Degradation of Thermal-Pretreated Oil Palm Empty Fruit Bunch. *Energies* **2020**, *13*, 5966. [CrossRef]
50. Senneca, O.; Cerciello, F.; Russo, C.; Wütscher, A.; Muhler, M.; Apicella, B. Thermal treatment of lignin, cellulose and hemicellulose in nitrogen and carbon dioxide. *Fuel* **2020**, *271*, 117656. [CrossRef]
51. Khamwichit, A.; Kasawapat, J.; Seekao, N.; Dechapanya, W. Enhanced Torrefied Oil-Palm Biomass as an Alternative Bio-Circular Solid Fuel: Innovative Modeling of Optimal Conditions and Ecoefficiency Analysis. *Energies* **2024**, *17*, 2192. [CrossRef]
52. Triviño-Pineda, J.-S.; Sanchez-Rodriguez, A.; Peláez, N.P. Biogas production from organic solid waste through anaerobic digestion: A meta-analysis. *Case Stud. Chem. Environ. Eng.* **2024**, *9*, 100618. [CrossRef]
53. Solarte-Toro, J.C.; Chacón-Pérez, Y.; Cardona-Alzate, C.A. Evaluation of biogas and syngas as energy vectors for heat and power generation using lignocellulosic biomass as raw material. *Electron. J. Biotechnol.* **2018**, *33*, 52–62. [CrossRef]
54. de Moraes, J.P.; Poço, J.G.R. Thermodynamical analysis of carbon activity in ethanol steam reforming. *Energy Convers. Manag.* **2024**, *317*, 118856. [CrossRef]
55. Zhong, Y.; Zhang, Y.; Mao, C.; Ukaew, A. Performance, Combustion, and Emission Comparisons of a High-Speed Diesel Engine Fueled with Biodiesel with Different Ethanol Addition Ratios Based on a Combined Kinetic Mechanism. *Processes* **2022**, *10*, 1689. [CrossRef]
56. Paone, E.; Tursi, A. Production of biodiesel from biomass. In *Advances in Bioenergy and Microfluidic Applications*; Elsevier: Amsterdam, The Netherlands, 2021; pp. 165–192. [CrossRef]
57. van Gelderen, L.; Alva, U.R.; Mindykowski, P.; Jomaas, G. Thermal Properties and Burning Efficiencies of Crude Oils and Refined Fuel Oil. *Int. Oil Spill Conf. Proc.* **2017**, *2017*, 985–1005. [CrossRef]
58. Chowdhury, H.; Chowdhury, T.; Hossain, N.; Chowdhury, P.; Salam, B.; Sait, S.M.; Mahlia, T.M.I. Exergetic sustainability analysis of industrial furnace: A case study. *Environ. Sci. Pollut. Res.* **2021**, *28*, 12881–12888. [CrossRef]
59. Peng, J.H.; Bi, H.T.; Sokhansanj, S.; Lim, J.C. A Study of Particle Size Effect on Biomass Torrefaction and Densification. *Energy Fuels* **2012**, *26*, 3826–3839. [CrossRef]
60. Ivanovski, M.; Goričanec, D.; Urbancl, D. The Evaluation of Torrefaction Efficiency for Lignocellulosic Materials Combined with Mixed Solid Wastes. *Energies* **2023**, *16*, 3694. [CrossRef]
61. Mamvura, T.; Danha, G. Biomass torrefaction as an emerging technology to aid in energy production. *Heliyon* **2020**, *6*, e03531. [CrossRef]
62. Díez, D.; Urueña, A.; Piñero, R.; Barrio, A.; Tamminen, T. Determination of Hemicellulose, Cellulose, and Lignin Content in Different Types of Biomasses by Thermogravimetric Analysis and Pseudocomponent Kinetic Model (TGA-PKM Method). *Processes* **2020**, *8*, 1048. [CrossRef]
63. Chen, W.-H.; Wu, J.-S. An evaluation on rice husks and pulverized coal blends using a drop tube furnace and a thermogravimetric analyzer for application to a blast furnace. *Energy* **2009**, *34*, 1458–1466. [CrossRef]
64. Zhang, S.; Li, R.; Zhang, Y.; Zhao, M. The effect of solvents on the thermal degradation products of two Amadori derivatives. *RSC Adv.* **2020**, *10*, 9309–9317. [CrossRef] [PubMed]
65. Rao, J.; Lv, Z.; Chen, G.; Peng, F. Hemicellulose: Structure, chemical modification, and application. *Prog. Polym. Sci.* **2023**, *140*, 101675. [CrossRef]
66. Gellerstedt, G.; Henriksson, G. Lignins: Major Sources, Structure and Properties. In *Monomers, Polymers and Composites from Renewable Resources*; Elsevier: Amsterdam, The Netherlands, 2008; pp. 201–224. [CrossRef]
67. Ong, H.C.; Yu, K.L.; Chen, W.-H.; Pillejera, M.K.; Bi, X.; Tran, K.-Q.; Pétrissans, A.; Pétrissans, M. Variation of lignocellulosic biomass structure from torrefaction: A critical review. *Renew. Sustain. Energy Rev.* **2021**, *152*, 111698. [CrossRef]
68. Houfani, A.A.; Anders, N.; Spiess, A.C.; Baldrian, P.; Benallaoua, S. Insights from enzymatic degradation of cellulose and hemicellulose to fermentable sugars—A review. *Biomass-Bioenergy* **2020**, *134*, 105481. [CrossRef]

69. Ivanovski, M.; Urbancl, D.; Petrovič, A.; Stergar, J.; Goričanec, D.; Simonič, M. Improving Lignocellulosic and Non-Lignocellulosic Biomass Characteristics through Torrefaction Process. *Appl. Sci.* **2022**, *12*, 12210. [CrossRef]
70. Okolie, J.A.; Nanda, S.; Dalai, A.K.; Kozinski, J.A. Chemistry and Specialty Industrial Applications of Lignocellulosic Biomass. *Waste Biomass-Valorization* **2020**, *12*, 2145–2169. [CrossRef]
71. Nam, H.; Capareda, S. Experimental investigation of torrefaction of two agricultural wastes of different composition using RSM (response surface methodology). *Energy* **2015**, *91*, 507–516. [CrossRef]
72. Waheed, A.; Naqvi, S.R.; Ali, I. Co-Torrefaction Progress of Biomass Residue/Waste Obtained for High-Value Bio-Solid Products. *Energies* **2022**, *15*, 8297. [CrossRef]
73. Simonic, M.; Goricanec, D.; Urbancl, D. Impact of torrefaction on biomass properties depending on temperature and operation time. *Sci. Total. Environ.* **2020**, *740*, 140086. [CrossRef] [PubMed]
74. Ahamed, M.; Perera, M.; Matthai, S.; Ranjith, P.; Dong-Yin, L. Coal composition and structural variation with rank and its influence on the coal-moisture interactions under coal seam temperature conditions—A review article. *J. Pet. Sci. Eng.* **2019**, *180*, 901–917. [CrossRef]
75. Skone, T.; Schivley, G.; Jamieson, M.; Marriott, J.; Cooney, G.; Littlefield, J.; Mutchek, M.; Krynock, M.; Shih, C. *Life Cycle Analysis: Supercritical Pulverized Coal (SCPC) Power Plants*; USDOE Office of Fossil Energy (FE): Albany, OR, USA, 2018. [CrossRef]
76. Business Insider, Coal-Price; Markets Insider. 2024. Available online: https://markets.businessinsider.com/commodities/coal-price (accessed on 20 September 2024).

Disclaimer/Publisher's Note: The statements, opinions and data contained in all publications are solely those of the individual author(s) and contributor(s) and not of MDPI and/or the editor(s). MDPI and/or the editor(s) disclaim responsibility for any injury to people or property resulting from any ideas, methods, instructions or products referred to in the content.